



National Library  
of Canada

Acquisitions and  
Bibliographic Services Branch

395 Wellington Street  
Ottawa, Ontario  
K1A 0N4

Bibliothèque nationale  
du Canada

Direction des acquisitions et  
des services bibliographiques

395, rue Wellington  
Ottawa (Ontario)  
K1A 0N4

*Your file - Votre référence*

*Our file - Notre référence*

## NOTICE

The quality of this microform is heavily dependent upon the quality of the original thesis submitted for microfilming. Every effort has been made to ensure the highest quality of reproduction possible.

If pages are missing, contact the university which granted the degree.

Some pages may have indistinct print especially if the original pages were typed with a poor typewriter ribbon or if the university sent us an inferior photocopy.

Reproduction in full or in part of this microform is governed by the Canadian Copyright Act, R.S.C. 1970, c. C-30, and subsequent amendments.

## AVIS

La qualité de cette microforme dépend grandement de la qualité de la thèse soumise au microfilmage. Nous avons tout fait pour assurer une qualité supérieure de reproduction.

S'il manque des pages, veuillez communiquer avec l'université qui a conféré le grade.

La qualité d'impression de certaines pages peut laisser à désirer, surtout si les pages originales ont été dactylographiées à l'aide d'un ruban usé ou si l'université nous a fait parvenir une photocopie de qualité inférieure.

La reproduction, même partielle, de cette microforme est soumise à la Loi canadienne sur le droit d'auteur, SRC 1970, c. C-30, et ses amendements subséquents.

Canada

Binding of  $\beta$ -Cyclodextrin and Hydroxypropyl- $\beta$ -Cyclodextrin to Alcohol

Yuqing Tan

A Thesis

in

The Department

of

Chemistry and Biochemistry

Presented in Partial Fulfillment of the Requirements

for the Degree of Master of Science at

Concordia University

Montreal, Quebec, Canada

March 1995

© Yuqing Tan, 1995



National Library  
of Canada

Bibliothèque nationale  
du Canada

Acquisitions and  
Bibliographic Services Branch

Direction des acquisitions et  
des services bibliographiques

395 Wellington Street  
Ottawa, Ontario  
K1A 0N4

395, rue Wellington  
Ottawa (Ontario)  
K1A 0N4

Your file    Votre référence

Our file    Notre référence

THE AUTHOR HAS GRANTED AN  
IRREVOCABLE NON-EXCLUSIVE  
LICENCE ALLOWING THE NATIONAL  
LIBRARY OF CANADA TO  
REPRODUCE, LOAN, DISTRIBUTE OR  
SELL COPIES OF HIS/HER THESIS BY  
ANY MEANS AND IN ANY FORM OR  
FORMAT, MAKING THIS THESIS  
AVAILABLE TO INTERESTED  
PERSONS.

L'AUTEUR A ACCORDE UNE LICENCE  
IRREVOCABLE ET NON EXCLUSIVE  
PERMETTANT A LA BIBLIOTHEQUE  
NATIONALE DU CANADA DE  
REPRODUIRE, PRETER, DISTRIBUER  
OU VENDRE DES COPIES DE SA  
THESE DE QUELQUE MANIERE ET  
SOUS QUELQUE FORME QUE CE SOIT  
POUR METTRE DES EXEMPLAIRES DE  
CETTE THESE A LA DISPOSITION DES  
PERSONNE INTERESSEES.

THE AUTHOR RETAINS OWNERSHIP  
OF THE COPYRIGHT IN HIS/HER  
THESIS. NEITHER THE THESIS NOR  
SUBSTANTIAL EXTRACTS FROM IT  
MAY BE PRINTED OR OTHERWISE  
REPRODUCED WITHOUT HIS/HER  
PERMISSION.

L'AUTEUR CONSERVE LA PROPRIETE  
DU DROIT D'AUTEUR QUI PROTEGE  
SA THESE. NI LA THESE NI DES  
EXTRAITS SUBSTANTIELS DE CELLE-  
CI NE DOIVENT ETRE IMPRIMES OU  
AUTREMENT REPRODUITS SANS SON  
AUTORISATION.

ISBN 0-612-01335-9

Canada

### **Abstract**

#### **Binding of $\beta$ -Cyclodextrin and Hydroxypropyl $\beta$ -Cyclodextrin to Alcohol**

**Yuqing Tan**

Cyclodextrins (CDs) are naturally occurring torus-shaped cyclic oligosaccharides made up of six, seven, or eight glucose units ( $\alpha$ -,  $\beta$ -,  $\gamma$ -CD, respectively) joined together by  $\alpha$ -1,4-glycosidic linkages. Hydroxypropyl- $\beta$ -cyclodextrin (HP- $\beta$ -CD) is  $\beta$ -CD that has its six primary hydroxyls alkylated. Because of their hydrophobic interiors CDs easily form host-guest inclusion complexes with a large variety of organic and inorganic compounds. The object of this research was to develop a method to determine the association constants of CD-guest complexes by reversed-phase HPLC, where CDs are injected and guests are used as mobile phase modifier. Association constants and stoichiometries for  $\beta$ -CD/2-propanol, HP- $\beta$ -CD/2-propanol,  $\beta$ -CD/t-butanol and HP- $\beta$ -CD/t-butanol have been obtained by this new method and are  $19.4 (\pm 6.4) \text{ M}^{-2}$  (1:2),  $1.7 (\pm 0.1) \text{ M}^{-2}$  (1:2),  $5.6 (\pm 0.7) \text{ M}^{-1}$  (1:1),  $2.2 (\pm 0.4) \text{ M}^{-1}$  (1:1), respectively. Values obtained by a spectroscopic displacement method that assumes 1:1 binding are  $6.1 (\pm 1.0) \text{ M}^{-1}$ ,  $0.8 (\pm 0.4) \text{ M}^{-1}$ ,  $45.6 (\pm 0.8) \text{ M}^{-1}$ ,  $2.0 (\pm 0.1) \text{ M}^{-1}$ , respectively. It is concluded that this new method can be used to determine both the association constants and the stoichiometries of CD-guest complexes.

**Dedicated to My Beloved Parents**

### **Acknowledgement**

I wish to thank my supervisor Dr. S. Mikkelsen and Dr. O.S. Tee for their guidance, assistance and encouragement throughout the course of this work.

I am also grateful to the following:

Dr. R.T. Rye and Dr. L.D. Colebrook for serving in my research committee.

All those individuals who have contributed to my knowledge and achievement.



<b>3. Determination of Association Constants of CD-Alcohol Complexes by a</b>	
<b>Reversed-Phase HPLC Method</b>	<b>45</b>
3.1 Introduction	45
3.2 Experimental	50
3.2.1 Reagents	50
3.2.2 Apparatus	50
3.2.3 Methods	50
3.2.3.1 Flow Injection	50
3.2.3.2 Reversed-Phase HPLC	51
3.3 Results and Discussion	51
3.4 References	64
<b>4. Summary and Suggestion for Future work</b>	<b>66</b>
Appendix	70



	<b><u>List of Figures</u></b>	<b>Page</b>
<b><u>Figure 1.1</u></b>	Structures of $\alpha$ , $\beta$ , $\gamma$ -cyclodextrin.	2
<b><u>Figure 1.2</u></b>	Dimensions of cyclodextrins.	3
<b><u>Figure 1.3</u></b>	Structure of ANS.	5
<b><u>Figure 2.1</u></b>	The excitation spectra of ANS.	24
<b><u>Figure 2.2</u></b>	The emission spectra of ANS.	24
<b><u>Figure 2.3</u></b>	Fluorescence emission spectra of ANS in the presence of $\alpha$ -CD.	25
<b><u>Figure 2.4</u></b>	Fluorescence emission spectra of ANS in the presence of $\beta$ -CD.	26
<b><u>Figure 2.5</u></b>	Fluorescence emission spectra of in ANS the presence of HP- $\beta$ -CD.	27
<b><u>Figure 2.6</u></b>	Scatchard plot of ANS- $\alpha$ -CD.	28
<b><u>Figure 2.7</u></b>	Scatchard plot of ANS- $\beta$ -CD.	28
<b><u>Figure 2.8</u></b>	Scatchard plot of ANS-HP- $\beta$ -CD.	29
<b><u>Figure 2.9</u></b>	Fluorescence intensity of ANS vs $\alpha$ -CD concentration.	29
<b><u>Figure 2.10</u></b>	Fluorescence intensity of ANS vs $\beta$ -CD concentration.	30
<b><u>Figure 2.11</u></b>	Fluorescence intensity of ANS vs HP- $\beta$ -CD concentration.	30
<b><u>Figure 2.12</u></b>	Fluorescence emission spectra of ANS- $\beta$ -CD in the presence of various concentrations of 2-propanol.	35
<b><u>Figure 2.13</u></b>	Fluorescence emission spectra of ANS- $\beta$ -CD in the presence of various concentrations of t-butanol.	36
<b><u>Figure 2.14</u></b>	Fluorescence emission spectra of ANS-HP- $\beta$ -CD in the presence of various concentrations of 2-propanol.	37

<b><u>Figure 2.15</u></b>	Fluorescence emission spectra of ANS- $\beta$ -CD in the presence of various concentrations of t-butanol.	38
<b><u>Figure 2.16</u></b>	Double reciprocal plot of $\Delta I$ and [2-propanol] for ANS- $\beta$ -CD.	39
<b><u>Figure 2.17</u></b>	Double reciprocal plot of $\Delta I$ and [t-butanol] for ANS- $\beta$ -CD.	39
<b><u>Figure 2.18</u></b>	Double reciprocal plot of $\Delta I$ and [2-propanol] for ANS-HP- $\beta$ -CD.	40
<b><u>Figure 2.19</u></b>	Double reciprocal plot of $\Delta I$ and [t-butanol] for ANS-HP- $\beta$ -CD.	40
<b><u>Figure 3.1</u></b>	Signal-to-background ratio vs log [ANS].	52
<b><u>Figure 3.2</u></b>	Chromatograms of HP- $\beta$ -CD at different concentrations of 2-propanol (A).	54
	Retention time of HP- $\beta$ -CD vs [2-propanol] (B).	54
<b><u>Figure 3.3</u></b>	Capacity factor $k'$ vs [guest].	55
<b><u>Figure 3.4</u></b>	Plot of $1/k'$ vs [2-propanol] for HP- $\beta$ -CD.	56
	Plot of $1/k'$ vs [2-propanol] <sup>2</sup> for HP- $\beta$ -CD.	56
<b><u>Figure 3.5</u></b>	Plot of $1/k'$ vs [2-propanol] for $\beta$ -CD.	57
	Plot of $1/k'$ vs [2-propanol] <sup>2</sup> for $\beta$ -CD.	57
<b><u>Figure 3.6</u></b>	Plot of $1/k'$ vs [t-butanol] for HP- $\beta$ -CD.	58
	Plot of $1/k'$ vs [t-butanol] <sup>2</sup> for HP- $\beta$ -CD.	
<b><u>Figure 3.7</u></b>	Plot of $1/k'$ vs [t-butanol] for $\beta$ -CD.	59
	Plot of $1/k'$ vs [t-butanol] <sup>2</sup> for $\beta$ -CD.	
<b><u>Figure 3.8</u></b>	Plot of $1/k'$ vs [2-propanol] for HP- $\beta$ -CD on phenyl column.	60

	<u>List of Tables</u>	Page
<u>Table 1.1</u>	Properties of $\beta$ -CD and its derivatives.	8
<u>Table 1.2</u>	Apparent binding constants for complexes of analytes with $\beta$ -CD and its derivatives.	10
<u>Table 2.1</u>	Association constants of cyclodextrins with alcohols.	18
<u>Table 2.2.</u>	$K_a$ values of ANS-CD complexes.	32
<u>Table 2.3</u>	$K_a$ Values for CD-alcohol complexes.	41
<u>Table 3.1</u>	$K_a$ values from reversed phase HPLC.	63
<u>Table 4.1</u>	Summary of $K_a$ values.	67

<b><u>List of Appendices</u></b>	<b>Page</b>
<b><u>Appendix 1</u></b> Linear regression (Scatchard Plot) method for $K_a$ determination.	70
<b><u>Appendix 2</u></b> Nonlinear regression method for $K_a$ determination.	73
<b><u>Appendix 3</u></b> Spectroscopic displacement method.	76
<b><u>Appendix 4</u></b> Fluorescence intensity of ANS with $\alpha$ -CD.	81
Fluorescence intensity of ANS with $\beta$ -CD.	82
Fluorescence intensity of ANS with HP- $\beta$ -CD.	83
<b><u>Appendix 5</u></b> Fluorescence intensity of ANS at different pH.	84
Fluorescence intensity of ANS- $\beta$ -CD at different pH.	85
Fluorescence intensity of ANS-HP- $\beta$ -CD at different pH.	86
<b><u>Appendix 6</u></b> Fluorescence intensity of HP- $\beta$ -CD-ANS in the presence of t-butanol.	87
Fluorescence intensity of $\beta$ -CD-ANS in the presence of t-butanol.	88
Fluorescence intensity of HP- $\beta$ -CD-ANS in the presence of 2-propanol.	89
Fluorescence intensity of $\beta$ -CD-ANS in the presence of 2-propanol.	90
<b><u>Appendix 7</u></b> RP-HPLC Method for $K_a$ determination.	91
<b><u>Appendix 8</u></b> Results from flow injection.	94
<b><u>Appendix 9</u></b> Retention times ( $C_{18}$ ) of HP- $\beta$ -CD in the presence of t-butanol.	95

Retention times ( $C_{18}$ ) of $\beta$ -CD in the presence of t-butanol.	96
Retention times ( $C_{18}$ ) of HP- $\beta$ -CD in the presence of 2-propanol.	97
Retention times ( $C_{18}$ ) of $\beta$ -CD in the presence of 2-propanol.	98
Retention times (Phenyl) of HP- $\beta$ -CD in the presence of 2-propanol.	99

## **1. Introduction**

### **1.1 Structure and Properties of Cyclodextrins<sup>1</sup>**

Cyclodextrins (CDs) are naturally occurring torus-shaped cyclic oligosaccharides made of six, seven, or eight glucose units joined by  $\alpha$ -1,4-glycosidic linkages, and they are referred to as  $\alpha$ -CD,  $\beta$ -CD and  $\gamma$ -CD, respectively (Figure 1.1)<sup>2</sup>. The hydrophilic hydroxyl groups are situated on both sides of the ring: primary hydroxyls on the narrower side and secondary hydroxyls on the wider sides. The free rotation of primary hydroxyl groups reduces the effective diameter of the cavity opening. The two hydroxyl groups of adjacent glucose units can form hydrogen bonds which stabilize the shape of the molecule and at the same time significantly influence its solubility in water. These hydroxyl groups account for the hydrophilic exterior of CDs. The CD cavity is defined by two rings of C-H groups and one ring of glucosidic oxygens, so the interior is much more hydrophobic than the exterior. Because of their hydrophobic cavities CDs readily form stable inclusion complexes with a variety of compounds. Because the CDs have different internal diameters (Figure 1.2)<sup>2</sup>, they are capable of selectively binding guests that possess the appropriate size and geometry.

### **1.2 Host-Guest Complexes of Cyclodextrins**

The driving forces for CD inclusion complex formation are proposed to be Van der Waals interactions between the guest and CD, hydrogen bonding between the guest

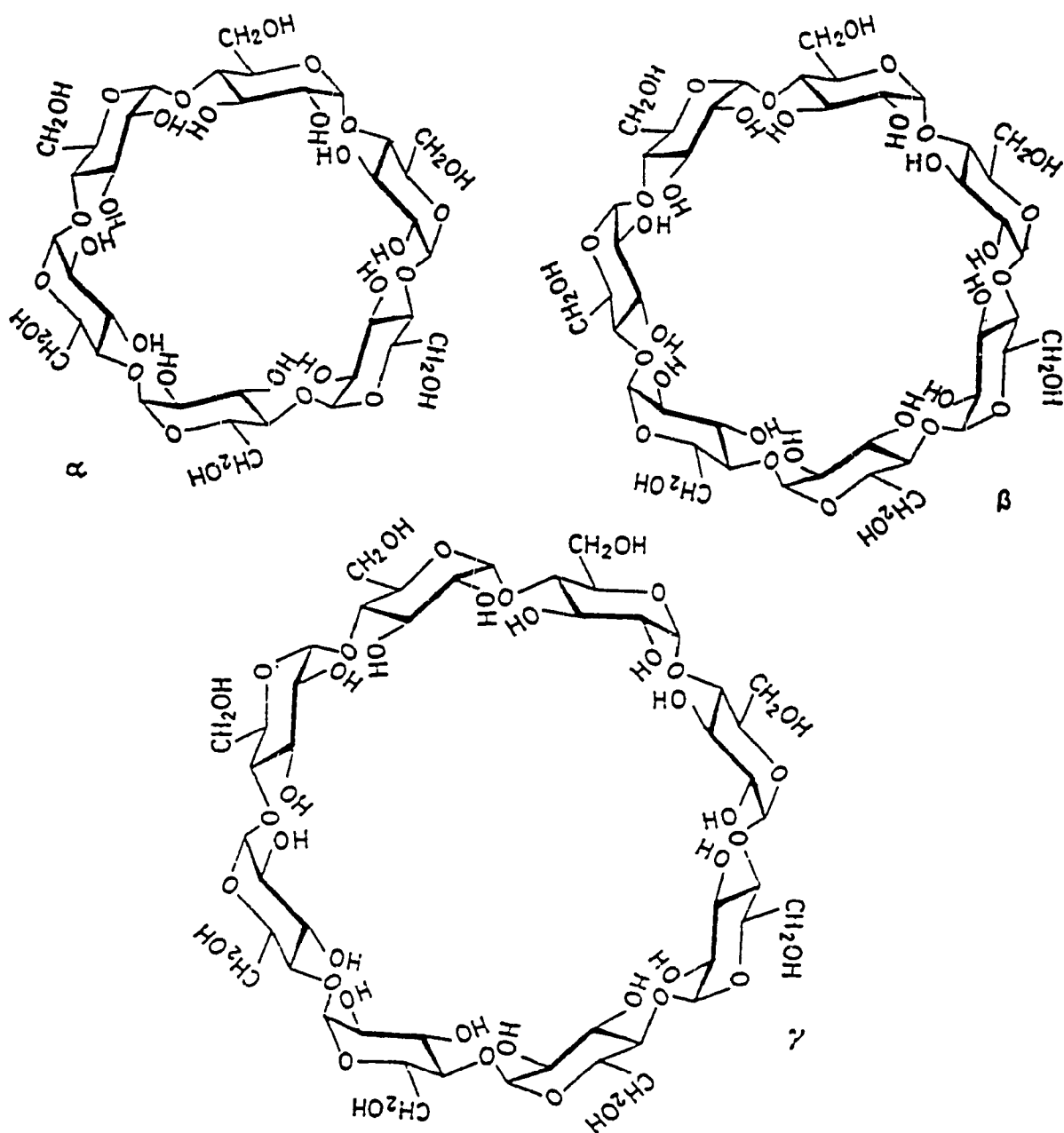


**Figure 1.1** Structures of  $\alpha$ ,  $\beta$ ,  $\gamma$ -cyclodextrin.

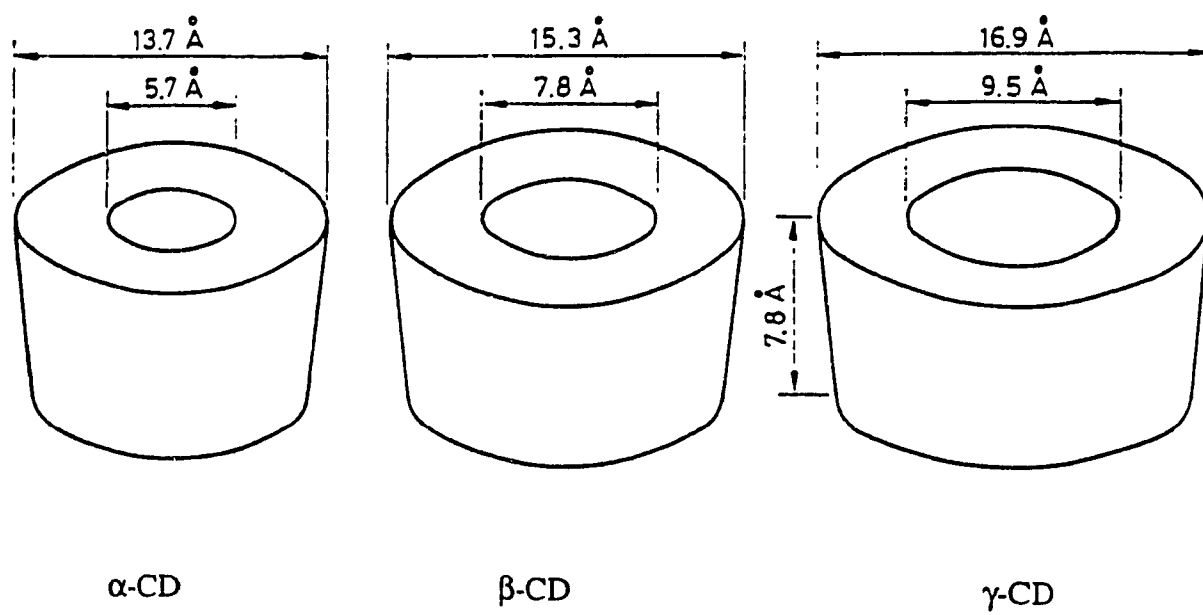


**Figure 1.2.** Dimensions of cyclodextrins.



and the hydroxyl groups of the CDs, the release of high energy water molecules that occurs upon complex formation, the release of strain energy in the macromolecular ring of the CDs and hydrophobic interactions between host and guest<sup>1</sup>. The strength of the host-guest complexes can be described by association constants.

Many methods have been developed to determine the association constants of host-guest complexes, and these methods can be classified as direct or indirect methods. Direct methods include UV-visible spectroscopy<sup>3,4</sup>, fluorometry<sup>5-9</sup>, conductimetry<sup>10</sup>, kinetics<sup>3,4,11</sup>, nuclear magnetic resonance spectrometry (NMR)<sup>12</sup> and reversed-phase high performance liquid chromatography (RP-HPLC)<sup>13-17</sup> methods. In all these methods the property of the guest is monitored directly. For example, 6-p-toluidinylnaphthlene-2-sulfonate (TNS) shows pronounced fluorescence enhancement upon addition of  $\alpha$ -CD,  $\beta$ -CD or  $\gamma$ -CD. The changes in fluorescence intensity allow determination of association constants of CD-TNS complexes<sup>6</sup>. When the guest is spectroscopically transparent the association constant of the CD-guest complex can be determined by an indirect method such as UV-visible spectroscopy<sup>3,18,19</sup>, fluorometry<sup>20</sup> and kinetic methods<sup>4,11,21</sup> by using a probe. For example, an alcohol (ROH) can affect the equilibrium of  $\alpha$ -CD or  $\beta$ -CD-azo-dye systems, and so affect the absorbance of the system at a certain wavelength. The changes in the absorbance can be used to determine the association constants of the alcohol with  $\alpha$ -CD and  $\beta$ -CD<sup>19</sup>.

Because the different cyclodextrins have different cavity sizes, their binding behaviour with the same guest is not the same. 1-Anilino-8-naphthalenesulfonate (ANS) (Figure 1.3) is frequently used as a fluorescent probe because its fluorescence is very

sensitive to the surrounding environment. For example, ANS exhibits only a very low fluorescence in water, but when ANS and a CD forms an inclusion complex, the ANS molecule is transported into a partially hydrophobic surrounding, and its fluorescence is dramatically increased. ANS binding to CDs of different size is not the same. For example, the association constants of ANS complexes with  $\alpha$ -CD<sup>12</sup>,  $\beta$ -CD<sup>5</sup> and  $\gamma$ -CD<sup>22</sup> are  $5\text{ M}^{-1}$ ,  $65\text{ M}^{-1}$  and  $1260\text{ M}^{-1}$ , respectively. The reason suggested by Schneider and co-workers by using NMR technique<sup>12</sup> is that although both  $\alpha$ -CD and  $\beta$ -CD include the aniline residue of ANS, ANS has more mobility in  $\beta$ -CD cavity, so ANS binding to  $\beta$ -CD is stronger;  $\gamma$ -CD have large enough internal diameters to enclose the naphthalenesulfonic residue and protect ANS from quenching processes better, so  $\gamma$ -CD binding to ANS is strongest of these three CDs. ANS can also be used as an indirect fluorescent probe to detect the interaction of CDs with a second guest<sup>20</sup>.

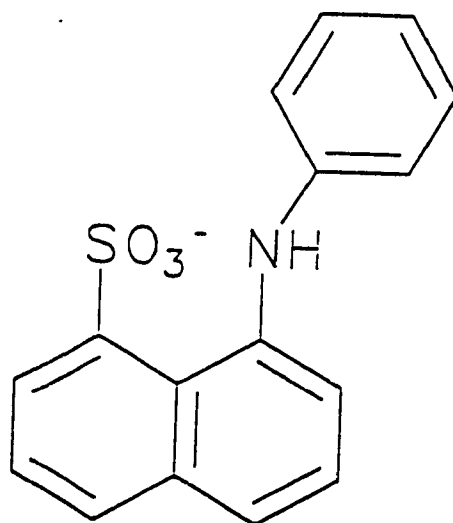


**Figure 1.3** Structure of ANS.

Normally 1:1 complex formation is assumed, but 2:1 complexes have been reported<sup>5,6 13,16</sup>. The apparent formation constants of  $\beta$ -CD or  $\gamma$ -CD with pyrene increase dramatically in the presence of the alcohols and this suggests that alcohol-CD-pyrene ternary complexes are formed<sup>23-26</sup>.

Because of their ability to form host-guest complexes, CDs have found numerous analytical and industrial applications<sup>2</sup>. They have been used to increase the sensitivity of quantitative analysis of some fluorophores<sup>8,9</sup>, such as dulcin [(4-ethoxyphenyl)urea] and pharmaceutical compounds. When the fluorophore is included in the CD cavity, the excited state is protected from quenching and non-radiative decay processes that easily occur in bulk aqueous solution, so a greater fluorescence emission intensity is observed. CDs have also been used in reversed-phase high performance liquid chromatography (RPLC) as mobile phase modifiers<sup>27-29</sup> or as a stationary phase<sup>30-32</sup> to separate a wide variety of structural, positional and optical isomers.

In basic aqueous solution the ionized secondary hydroxyl groups of CDs can act as a nucleophile to bring about ester cleavage. For example, the cleavage of *m*-nitrophenyl acetate is accelerated by a factor of 70 by  $\alpha$ -CD. This is because  $\alpha$ -CD binds the substrate molecule in a favourable orientation for the reaction to occur, i.e., the ester group is oriented towards the nearby secondary hydroxyls, so this kind of nucleophilic attack is more efficient than general base catalysis<sup>2</sup>. Because CDs have the apolar cavity as a substrate binding site, hydroxyl groups as the active site and the formation of a covalent intermediate in these reactions, CDs can be used as enzyme models to study the mechanisms of biological reactions. Also since the cavity of cyclodextrins has a definite

size and shape, like enzymes, CDs can catalyze hydrolytic reactions selectively .

$\beta$ -CD is of particular interest in the pharmaceutical industry. It is relatively inexpensive, has an intermediate cavity size and enhances the solubility, dissolution rate, stability and bioavailability of various small drug species, through host-guest complex formation<sup>2,13</sup>. The binding properties of  $\beta$ -CD and its derivatives are therefore of great potential use in the pharmaceutical industry.

Although  $\beta$ -CD has been studied widely, its application is limited by its water solubility. From this point of view more water-soluble modified  $\beta$ -CDs may be recommended as fluorescence enhancement agents or as chromatographic mobile-phase modifiers. Furthermore, modified CDs can be better enzyme models by the introduction of specific groups to native CDs<sup>1</sup>.

### 1.3 Chemically-Modified Cyclodextrins

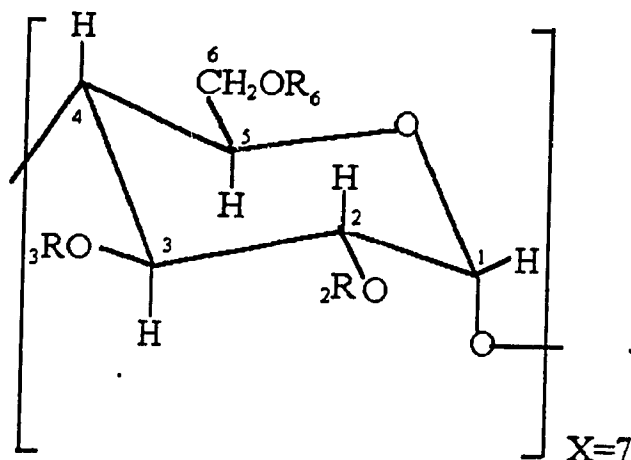
Recent studies have shown that modified cyclodextrins have some advantages over native cyclodextrins. The differences in molecular structures and physicochemical properties between  $\beta$ -CD and some water-soluble  $\beta$ -CD derivatives are shown in Table 1.1. Their binding constants with several analytes are listed in Table 1.2. Experiments have shown that more water-soluble  $\beta$ -CD derivatives resulted in a greater fluorescence from the analyte compared to that obtained with native  $\beta$ -CD. It is suggested that the enhanced fluorescence is due to a greater fraction of the solute molecules included within the protective cyclodextrin cavity because more concentrated water-soluble  $\beta$ -CD derivatives were used. The fluorescence enhancement allows more accurate determination of lower analyte concentrations<sup>9</sup>. In addition, the stability of a particular fluorescence

**Table 1.1** Properties of  $\beta$ -CD and Its Derivatives<sup>a</sup>

	Substituent(s) <sup>b</sup>	av molar substitution <sup>c</sup>	av molecular mass <sup>d</sup>	solubility in water at 25.0°C, M
native- $\beta$ -CD	$R_6=R_2=R_3=H$		1135	0.0163
HP- $\beta$ -CD	replacement of R's=H with one or more $-CH_2CH(OH)CH_3$	1.03	$1552 \pm 41$	$>0.40$
HE- $\beta$ -CD	replacement of R's=H by one or more $-CH_2CH_2OH$ moieties	0.51	$1293 \pm 18$	0.464
DOM- $\beta$ -CD	$R_6=R_2=CH_3$ ; $R_3=H$	2.06	1331	0.428

<sup>a</sup> Data taken from ref. 9.

<sup>b</sup> Refers to the substituents,  $R_6$ ,  $R_2$ , and  $R_3$ , on one glucose unit of the  $\beta$ -cyclodextrin molecule as shown:



<sup>c</sup> Average molar substitution of derivatized  $\beta$ -CD is defined as the average number of substitution on one glucose unit of native  $\beta$ -CD and calculated by using formula degree of substitution =  $\Sigma (\text{peak height} \times \text{the number of substituents}) / \Sigma \text{peak height}$ . For example the value of 1.03 for HP- $\beta$ -CD means that 1.03 hydroxyl groups out of three in native  $\beta$ -CD are substituted by hydroxypropyl groups (or a total of 7.2 such groups per one cyclodextrin molecule). Both molecular weight and degree of substitution of  $\beta$ -CD derivatives can be determined by mass spectrometry.

<sup>d</sup> modified  $\beta$ -CDs contain several components with various degree of substitution instead of a single product, and these components are distributed around the average molecular mass.

**Table 1.2** Apparent Binding Constants for Complexes of Analytes with  $\beta$ -CD and Its derivatives<sup>a</sup>

Analyte	$K_b, M^{-1}$			
	$\beta$ -CD	HP- $\beta$ -CD	HE- $\beta$ -CD	DOM- $\beta$ -CD
diazepam	220	138	140 <sup>b</sup>	770 <sup>b</sup>
digoxin	11000 <sup>b</sup>	7300 <sup>b</sup>	5600 <sup>b</sup>	37000 <sup>b</sup>
p-aminobenzoic acid	290	388		
indole	21	175	114	
phenolphthalein	22000 <sup>c</sup>	23500 <sup>c</sup>		
$C_6H_5CH(CH_3)CO_2-p-NO_2C_6H_5$	588 <sup>d</sup>			3300 <sup>d</sup>
ethyl-4-biphenyl acetate	3000 <sup>b</sup>	4100 <sup>b</sup>	2400 <sup>b</sup>	12500 <sup>b</sup>

<sup>a, b, c, d</sup> Data taken from ref. 9, ref. 34, ref. 35, ref. 36, respectively.

system was found increased when HP- $\beta$ -CD or DOM- $\beta$ -CD were used<sup>9</sup>. From the results listed in Table 1.2, the authors suggested that both steric and hydrophobic effects are involved in complexation process. It was reported that because HP- $\beta$ -CD and native  $\beta$ -CD have different structures they have different complexing properties when they include compounds with different size such as pyrene and naphthalene<sup>37</sup>. Although pyrene can be included by native  $\beta$ -CD, pyrene entry into the HP- $\beta$ -CD cavity is less favorable because the bulky hydroxypropyl groups effectively reduce the entrance diameter. For a smaller guest like naphthalene, HP- $\beta$ -CD shows a greater fluorescence enhancement than native  $\beta$ -CD. The authors suggested that the HP- $\beta$ -CD can prevent a bulky guest from completely entering the CD cavity, but can offer better protection to smaller guests. In this situation the steric effect is more important than hydrophobic effect.

Because CDs have been shown to possess an enzyme-like binding capacity for small organic molecules<sup>1</sup>, CDs have been derivatized with flavin groups to produce synthetic flavoenzymes and shown to be efficient in electron-transfer and redox reactions<sup>38</sup>.

Since modified  $\beta$ -CD species are of interest in complexation and catalysis, further work on the binding properties of modified  $\beta$ -CD species is significant.

#### **1.4 Objective**

Chromatographic separation results from selective binding of cyclodextrins of guests when CDs are used as mobile phase modifiers. The retention time of the guest decreases significantly in the presence of CD, because unretained CD-guest complexes are formed. The changes in the guest retention time with CD concentration are related



to the stability of the complex, and these data allow the determination of host-guest association constants for injected guest species<sup>11</sup>. This method has not been tested under conditions where the guest species is present in the mobile phase and CDs are injected.

It has been considered for a long time that CDs do not interact with reversed phase columns due to their hydrophilic exteriors. But recent studies<sup>19,40</sup> have shown that native CDs can be retained on octadecyl (C<sub>18</sub>) stationary phase, and can be well-resolved using mobile phases containing low concentrations of modifiers like acetonitrile or methanol. The objective of these experiments was to develop a chromatographic method to determine the association constants and binding stoichiometries for the reactions of CDs with guests, where CDs are the injected species. By injecting CD, and monitoring its retention time as a function of mobile-phase guest concentration, it should be possible to extend this chromatographic method to the study of CD derivative mixtures. In this way, binding data could be obtained for a number of different CD derivatives without a prior purification step. With complex mixture of CD derivatives, mass spectrometric detection could be used to identify individual CD species as they elute.

In this work, an accepted spectroscopic displacement method and the new RP-HPLC method were compared for the determination of association constants of CD-alcohol complexes.

## 1.5 References

- (1) Bender, M. L.; Komiyama, M. *Cyclodextrin Chemistry*; Springer-Verlag: New York, 1978.
- (2) Szejtli, J. *Cyclodextrins and Their Inclusion Complexes*; Akademiai kiado: Budapest, 1982.
- (3) Cramer, F.; Saenger, W.; Spatz, H.-Ch. *J. Am. Chem. Soc.*, **1967**, 89, 14-20.
- (4) VanEtten, R. L.; Sebastian, J. F.; Clowes, G. A.; Bender, M. L. *J. Am. Chem. Soc.*, **1967**, 89, 3242-3253.
- (5) Catena, G. C.; Bright, F. V.; *Anal. Chem.* **1989**, 61, 905-909.
- (6) Kondo, H.; Nakatani, H.; Hiromi, K. *J. Biochem.*, **1976**, 79, 393-405.
- (7) Aoyama, Y.; Nagai, Y.; Otsuki, J.-I.; Kobayashi, K.; Toi, H. *Tetrahedron Letters*. **1992**, 33, 3775-3778.
- (8) Navas Díaz, A.; Sánchez Fera, L.; García Sanchez, F. *Talanta*, **1994**, 41, 509-514.
- (9) Frankewich, R. P.; Thimmaiah, K. N.; Hinze, W. L. *Anal. Chem.*, **1991**, 63, 2924-2933.
- (10) Lavandier, C. D.; Pelletier, M. P.; Reinsborough, V. C. *Aust. J. Chem.*, **1991**, 44, 457-461.
- (11) Tee, O. S.; Gadosy, T. A.; Giorgi, J. B. *J. Chem. Soc., Perkin Trans. 2*, **1993**, 1705-1706.
- (12) Schneider, H.-J.; Blatter, T.; Simova, S. *J. Am. Chem. Soc.*, **1991**, 113, 1996-2000.
- (13) Anigbogu, V. C.; Muñoz de la Peña, A.; Ndou, T. T.; Warner, I. M. *Anal. Chem.*,

- 1992, 64, 484-489.
- (14) Uekama, K.; Hirayama, F.; Nasu, S.; Matsuo, N.; Irie, T. *Chem. Pharm. Bull.*, **1978**, 26, 3477-3484
- (15) Fujimura, K.; Ueda, T.; Kitagawa, M.; Takayanagi, H.; Ando, T. *Anal. Chem.*, **1986**, 58, 2668-2674.
- (16) Husain, N.; Anigbogu, V. C.; Cohen, M. R.; Warner, I. M. *J. Chromatogr.*, **1993**, 635, 211-219.
- (17) Armstrong, D. W.; Nome, F.; Spino, L. A.; Golden, T. D. *J. Am. Chem. Soc.*, **1986**, 108, 1418-1421.
- (18) Selvidge, L. A.; Eftink, M. R. *Anal. Biochem.*, **1986**, 154, 400-408.
- (19) Matsui, Y.; Mochida, K. *Bull. Chem. Soc. Jpn.*, **1979**, 52, 2808-2814.
- (20) Aoyama, Y.; Nagai, Y.; Otsuki, J.-I.; Kobayashi, K.; Toi, H. *Angew. Chem. Int. Ed. Engl.*, **1992**, 31, 745-747.
- (21) Demont, P. M.; Reinsborough, V. C. *Aust. J. Chem.*, **1991**, 44, 759-763.
- (22) Kumar, S.; Schneider, H.-J. *J. Chem. Soc., Perkin Trans. 2*. **1989**, 245.
- (23) Zung, J. B.; Muñoz de la Peña, A.; Ndou, T. T.; Warner, I. M. *J. Phys. Chem.*, **1991**, 95, 6701-6706.
- (24) Muñoz de la Peña, A.; Ndou, T. T.; Zung, J. B.; Greene, K. L.; Live, D. H.; Warner, I. M. *J. Am. Chem. Soc.*, **1991**, 113, 1572-1577.
- (25) Nelson, G.; Patonay, G.; Warner, I. M. *Talanta*, **1989**, 36, 199-203.
- (26) Nelson, G.; Patonay, G.; Warner, I. M. *Anal. Chem.*, **1988**, 60, 274-279.
- (27) Sybliska, D.; Asztemborska, M.; Bielejewska, A.; Kowalczyk, J.; Dodziuk, H.;

- Duszczyk, K.; Lamparczyk, H.; Zarzycki, P. *Chromatographia*, **1993**, *35*, 637-642.
- (28) Zukowski, J.; Sybilska, D.; Jurczak, J. *Anal. Chem.*, **1985**, *57*, 2215-2219.
- (29) Sybilska, D.; Lipkowski, J.; Woycikowski, J. *J.Chromotogr.*, **1982**, *253*, 95-100
- (30) Gazdag, M.; Szepesi, G.; Huszar, L. *J.Chromatogr.*, **1986**, *371*, 227.
- (31) Armstrong, R. D.; Armsrong, D. W.; War d, T. J.; Pattabiraman, N.; Benz, C. *J. Chromatogr.*, **1987**, *414*,192.
- (32) Armstrong, D. W.; Stalcup, A. M.; Chang, S-C. *J.Chromatogr.*, **1991**, *540*, 113.
- (33) Duchene, D.; Wouessidjewe, D. *J. Coord. Chem.*, **1992**, *27*, 223-236.
- (34) Yoshida, A.; Arima, H.; Uekama, K.; Pitha, J. *Int. J. Pharm.*, **1988**, *46*, 217-222
- (35) Rao, C. T.; Lindberg, B.; Lindberg, J.; Pitha, J. *J. Org. Chem.*, **1991**, *56*, 1327-1329.
- (36) Fornasier, R.; Reniero, F.; Scrimin, P.; Tonellato, U. *J. Chem. Soc., Perkin Trans. 2*, **1987**, 1121-1123.
- (37) Zung, J. B.; Ndou, T. T.; Warner, I. M. *Applied Spectroscopy*, **1990**, *44*, 1491-1493.
- (38) Rong, D.; Ye, H-P.; Boehlow, T. R.; D'souza, V.T. *J. Org. Chem.*, **1992**, *57*, 163-167
- (39) Koizumi, K.; Kubota, Y.; Okada, Y.; Utamura, T. *J.Chromatogr.*, **1988**, *437*, 47-57.
- (40) Haginaka, J.; Nishimura, Y.; Wakai, J.; Yasuda, H. *Anal. Biochem.* **1989**, *179*, 336-340.

## **2. Determination of Cyclodextrin-Guest Association Constants by Fluorescence**

### **Spectroscopy**

#### **2.1 Introduction**

Many methods have been used to determine the association constants of host-guest complexes of cyclodextrins (CDs), including absorbance<sup>1</sup> and fluorescence spectroscopy<sup>2,3,4</sup>, kinetics<sup>1,5</sup>, conductimetry<sup>6</sup>, NMR<sup>7</sup>, reversed-phase liquid chromatography (RPLC)<sup>8-11</sup> and others<sup>12</sup>. If the guest undergoes a significant change in absorption or fluorescence properties when it binds to a CD, a direct method can be used to determine the association constant for the reaction. For example<sup>13</sup>, at pH 10, phenolphthalein absorbs maximally at 550 nm with a molar absorptivity of  $3.7 \times 10^4 \text{ M}^{-1} \text{ cm}^{-1}$ . When phenolphthalein is bound to  $\beta$ -CD ( $K_a = 1.0 \times 10^4 \text{ M}^{-1}$ ), there is no shift in maximum wavelength, but the molar absorptivity at 550 nm decreases by about 65%. The fluorescent species 8-anilino-1-naphthalenesulfonate (ANS) shows a large increase in emission intensity, and a blue-shift in emission wavelength, when CDs are present in solution<sup>1</sup>. For these species, the direct measurement of absorption or fluorescence can be used to quantitate their reactions with CDs.

If the guest does not undergo a spectral change upon binding to CDs, an indirect method can be used, such as the spectroscopic displacement method<sup>13-15</sup>. In this method, a probe species, such as phenolphthalein or ANS, is used. The guest is added to the

probe-CD system, resulting in competition between the probe and guest for CD, and the displacement of probe produces a spectral change. A spectroscopic displacement method has been used to evaluate the association constants of CDs with alcohols using an absorbing azo dye as a probe, by monitoring the inhibitory effect of alcohol on the association of CD with the azo dye<sup>15</sup>. The addition of saturated aliphatic compounds, including primary, secondary and tertiary, alicyclic or aromatic alcohols to a solution containing  $\alpha$ -CD and sodium 4-(4-hydroxyl-1-naphthylazo)-1-naphthalenesulfonate or  $\beta$ -CD and methyl orange resulted in an increase in absorbance and indicated that alcohol is included by the CD at the expense of the azo dye. By this method association constants were obtained for the complexation of  $\alpha$ -CD and  $\beta$ -CD with a variety of alcohols, and a representative list of these values is given in Table 2.1. Association constants are seen to increase with chain length for primary aliphatic alcohols, illustrating the importance of hydrophobic interactions in CD-guest complexes.

Methods based on absorbance and fluorescence spectroscopy normally assume that guests bind CDs with 1:1 stoichiometry. Recent studies have shown, however, that ternary complexes are possible<sup>4,16,17,18,19</sup>. These complexes may have 1:2 or 2:1 CD-guest stoichiometry. Tee and co-workers studied the kinetics of phenyl ester cleavage in the presence of  $\alpha$ -CD or  $\beta$ -CD, and found that short chain esters mainly react through a 1:1 CD-ester complex, but for longer chains the ester exhibits an 2:1 (CD:ester) binding also. The authors suggested that the first binding involves inclusion of alkanoate chain and the second involves the aryl group<sup>19</sup>.

In this chapter, the association constants for the reaction of ANS with  $\alpha$ -CD,  $\beta$ -CD

**Table 2.1** Association Constants of Cyclodextrins with Alcohols<sup>a</sup>

Alcohols	$K_a \text{ M}^{-1}$	
	$\alpha\text{-CD}^b$	$\beta\text{-CD}^c$
Methanol	0.93	0.32
Ethanol	5.62	0.93
1-Propanol	23.4	3.71
2-Propanol	4.90	3.80
1-butanol	89.1	16.6
2-Methyl-2-propanol	4.36	47.9
1-Pentanol	323	63.1
1-Hexanol	891	219
1-Heptanol	$2.29 \times 10^3$	708
1-Octanol	$6.31 \times 10^3$	$1.48 \times 10^3$
Cyclobutanol	38.9	$1.48 \times 10^3$
cyclopentanol	45.7	120

<sup>a</sup> Data taken from ref. 15.

<sup>b</sup> An azo dye, sodium 4-(4-hydroxy-1-naphthylazo)-1-naphthalenesulfanate, was used as a probe .

<sup>c</sup> An azo dye, methyl orange, was used as a probe.

and hydroxypropyl  $\beta$ -CD (HP- $\beta$ -CD) are determined by direct fluorescence measurements. ANS is then used as a probe to determine the association constants of 2-propanol and *t*-butanol with  $\beta$ -CD and HP- $\beta$ -CD, by a fluorescence displacement method.

## 2.2 Experimental

### 2.2.1 Apparatus

Fluorescence measurements were performed on a Shimadzu spectrofluorimeter at  $25 (\pm 1) ^\circ\text{C}$ . The excitation wavelength was varied from 200 nm to 400 nm while emission wavelength was monitored from 400 nm to 600 nm.

*The spectral parameters for the determination of association constants of ANS with  $\alpha$ -CD,  $\beta$ -CD and HP- $\beta$ -CD.* The wavelengths for emission measurements were 494.4 nm, 490.0 nm and 468.0 nm for  $\alpha$ -CD,  $\beta$ -CD and HP- $\beta$ -CD, respectively. Excitation at 368.0 nm was used for all systems. Excitation and emission band widths for  $\alpha$ -CD,  $\beta$ -CD and HP- $\beta$ -CD were 5.0 nm and 5.0 nm, 5.0 nm and 5.0 nm, and 1.5 nm and 3.0 nm, respectively.

*The spectral parameters for the determination of association constants of 2-propanol or *t*-butanol with  $\beta$ -CD and HP- $\beta$ -CD* For  $\beta$ -CD-alcohol reactions, excitation and emission wavelengths of 368.0 nm and 490.0 nm were used, with excitation and emission band widths of 5.0 nm and 3.0 nm, respectively. For HP- $\beta$ -CD-alcohol reactions, excitation and emission wavelengths of 368.0 nm and 468.0 nm were used, with excitation and emission band widths of 1.5 nm and 3.0 nm, respectively.

The fluorescence intensity of the blank (distilled, deionized water) was subtracted from that of the sample.



### 2.2.2 Materials

$\alpha$ -CD,  $\beta$ -CD, HP- $\beta$ -CD (degree of substitution = 0.8) and 1-anilino-8-naphthalenesulfonate (ANS) were from Aldrich. Acetic acid and sodium acetate were from Baker. t-Butanol was obtained from Aldrich and 2-propanol (99.5%) was from Sigma-Aldrich.  $\beta$ -CD and HP- $\beta$ -CD (degree of substitution = 0.9) were obtained from Wacker were used for t-butanol experiments. These reagents were used as received. Distilled, deionized water was used to prepare solutions.

### 2.2.3 Methods

*Preparation of solutions for determination of association constants of ANS with of  $\alpha$ -CD,  $\beta$ -CD and HP- $\beta$ -CD.* Stock solutions of  $\alpha$ -CD,  $\beta$ -CD and HP- $\beta$ -CD were  $1.00 \times 10^{-2}$  M, 0.120 M and  $1.00 \times 10^{-2}$  M, respectively. The stock solution of ANS was  $1.00 \times 10^{-3}$  M. For each measured sample, 2.5 ml of the stock solution of ANS and different volumes of CD stock solutions were taken into a 25 ml volumetric flask and diluted to volume.

*Preparation of solutions for determination of association constants of 2-propanol or t-butanol with of  $\beta$ -CD and HP-  $\beta$ -CD.* Stock solutions of ANS,  $\beta$ -CD, HP- $\beta$ -CD, propanol and t-butanol were  $1.00 \times 10^{-3}$  M,  $1.50 \times 10^{-2}$  M, 0.10 M, 2.60 M and 1.25 M respectively. The concentrations of ANS and CDs were held constant in samples while the alcohol concentrations were varied:  $[\text{ANS}]_{\text{T}} = 1.00 \times 10^{-4}$  M,  $[\beta\text{-CD}]_{\text{T}} = 4.20 \times 10^{-3}$  M, and  $[\text{HP-}\beta\text{-CD}]_{\text{T}} = 8.00 \times 10^{-3}$  M. 2.5 ml ANS stock solution, 7 ml  $\beta$ -CD stock solution or 2 ml HP- $\beta$ -CD stock solution and different volume of propanol or t-butanol stock solution were taken into a 25 ml volumetric flask, and diluted to volume.

*Determination of ANS-CD association constants.* ANS and  $\beta$ -CD are assumed to form a 1:1 inclusion complex. The total concentration of ANS is much smaller than that of CD, so the equilibrium concentration of free CD can be assumed to be equal to the total concentration of CD. Two methods were used to calculate the association constants of ANS with  $\alpha$ -CD,  $\beta$ -CD and HP- $\beta$ -CD from fluorescence intensities measured at the emission wavelength of the complex: a linear regression method (the Scatchard Plot, Appendix 1) and a non-linear regression method (Appendix 2).

The linear regression (Scatchard) method is based on the following equation

$$\Delta I/[CD]_0 = K_a C[ANS]_0 - K_a \Delta I, \quad (1)$$

where  $\Delta I$  is the observed fluorescence intensity in the presence of CD minus the fluorescence intensity in the absence of CD.  $K_a$  is the association constant for the reaction of ANS with CD (eq. 2),



and  $K_a = [CD-ANS] / [ANS][CD]$ .  $C$  is a constant under the experimental conditions,  $[ANS]_0$  is total concentration of ANS, and  $[CD]_0$  is the total concentration of CD. A plot of  $\Delta I/[CD]_0$  versus  $\Delta I$  should give a straight line with a slope of  $-K_a$ .

The non-linear regression method is based on the relationship between the fluorescence intensity and the concentration of the CD shown below:

$$I = (I_0 K_d + I_b [CD]_0) / (K_d + [CD]_0) \quad (3)$$

where  $I_0$  is the fluorescence in absence of CD and  $I_b$  is the fluorescence ANS bound to CD,  $[CD]_0$  is the total concentration of CD, and  $K_d$  is the dissociation constant for the reaction shown in eq. 2. In this method  $K_d$ ,  $I_0$  and  $I_b$  are considered parameters. The non-linear regression program begins with proposed values for the three parameters in equation (3), and the values of these parameters are adjusted iteratively until the selected equation fits the data best by minimizing the residual sum of squares of its deviations with 95% confidence.

*Determination of alcohol-CD association constants.* ANS is used as a fluorescent probe. It is assumed that the CDs form complexes with both alcohol and ANS with 1:1 molar ratios and that alcohols compete with ANS for CD cavities. Based on these competitive equilibria, an equation can be obtained to evaluate the association constants (Appendix 3):

$$\frac{1}{\Delta I} = \frac{K_d' (K_d + [CD]_0)^2}{B K_d [ANS]_0 [CD]_0} \frac{1}{[guest]_0} + \frac{K_d + [CD]_0}{B [ANS]_0 [CD]_0}, \quad (4)$$

where  $[ANS]_0$  and  $[CD]_0$  are total concentrations of ANS and CD, respectively,  $K_d'$  is the dissociation constant for the reaction of CD-alcohol complex,  $K_d$  is the dissociation constant for the reaction of CD-ANS complex,  $B$  is a constant under the experimental conditions, and  $[guest]_0$  is the total concentration of the alcohol (either 2-propanol or t-

butanol).

From equation 4, a plot of  $1/\Delta I$  versus  $1/[\text{guest}]_0$  should give a straight line. The association constant  $K_d'$  can then be calculated from eq. 5:

$$K_d' = K_d / (K_d + [\text{CD}]_0) * \text{slope/intercept}, \quad (5)$$

where  $K_d$  and  $[\text{CD}]_0$  are known.

## 2.3 Results and Discussion

### 2.3.1 Fluorescence Properties of ANS

ANS is used as fluorescence probe because its fluorescence intensity and emission wavelength are very sensitive to the surrounding environment. In the absence of CD, ANS exhibits a small fluorescence signal with an excitation wavelength of 368.0 nm and emission wavelength of 512.0 nm. ANS exhibits enhanced fluorescence upon addition of CD ( $1.0 \times 10^{-2}$  M  $\alpha$ -CD,  $\beta$ -CD or HP- $\beta$ -CD), because it is included in the hydrophobic cavity of the CD. Figure 2.1 and 2.2 show the excitation and emission spectra of ANS in aqueous solution in the absence and presence of CDs. With the same concentration of CDs, the increase in emission intensity is about 2.0-fold, 10-fold and 230-fold for  $\alpha$ -CD,  $\beta$ -CD and HP- $\beta$ -CD, respectively, so the ability of different CDs to form inclusion complexes and/or the environment of the complexed ANS is different. To describe the binding quantitatively, the association constants were determined.

### 2.3.2 Association of ANS with $\alpha$ -CD, $\beta$ -CD and HP- $\beta$ -CD

Figure 2.3, 2.4 and 2.5 show the spectra of ANS at varying concentrations of  $\alpha$ -

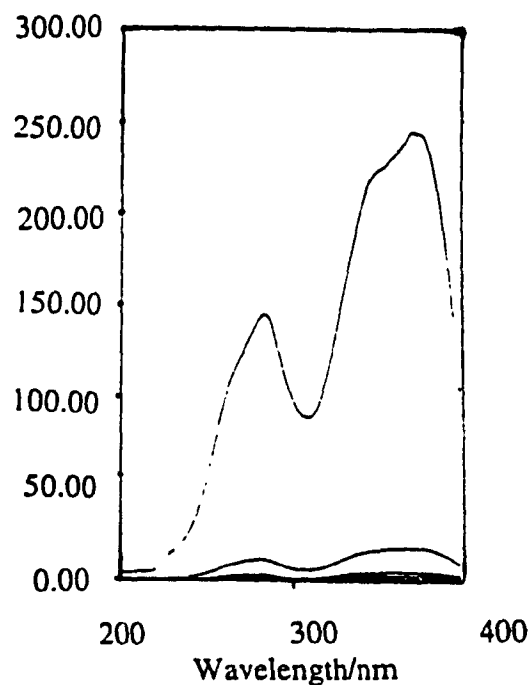


**Figure 2.1** The excitation spectra of  $1.0 \times 10^{-4}$  M ANS. From bottom to top 1) without CDs ( $\lambda_{em} = 512.0$  nm). 2)  $1.0 \times 10^{-2}$  M  $\alpha$ -CD ( $\lambda_{em} = 494.4.0$  nm). 3)  $1.0 \times 10^{-2}$  M  $\beta$ -CD ( $\lambda_{em} = 490.0$  nm). 4)  $1.0 \times 10^{-2}$  M HP- $\beta$ -CD ( $\lambda_{em} = 468.0.0$  nm). Excitation and emission band widths were 1.5 nm and 3.0 nm, respectively.

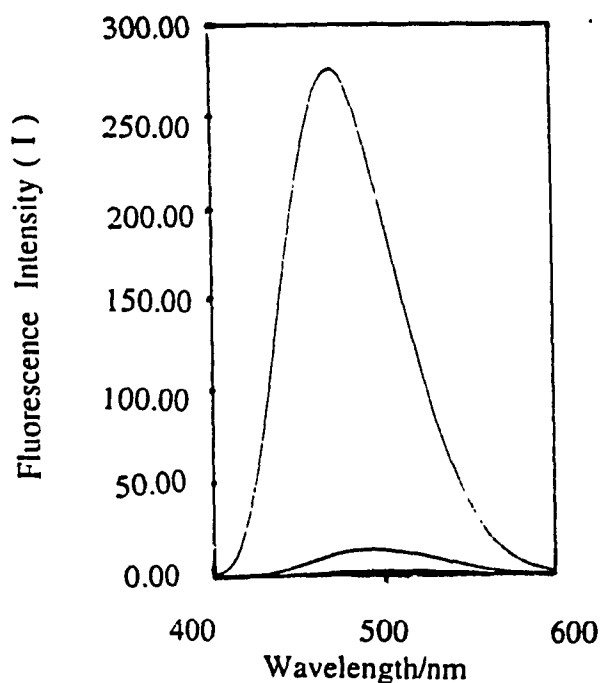


**Figure 2.2** The emission spectra of  $1.0 \times 10^{-4}$  M ANS. From bottom to top 1) without CDs. 2)  $1.0 \times 10^{-2}$  M  $\alpha$ -CD. 3)  $1.0 \times 10^{-2}$  M  $\beta$ -CD. 4)  $1.0 \times 10^{-2}$  M HP- $\beta$ -CD.  $\lambda_{ex} = 368.0$  nm. Excitation and emission band widths were 1.5 nm and 3.0 nm, respectively.

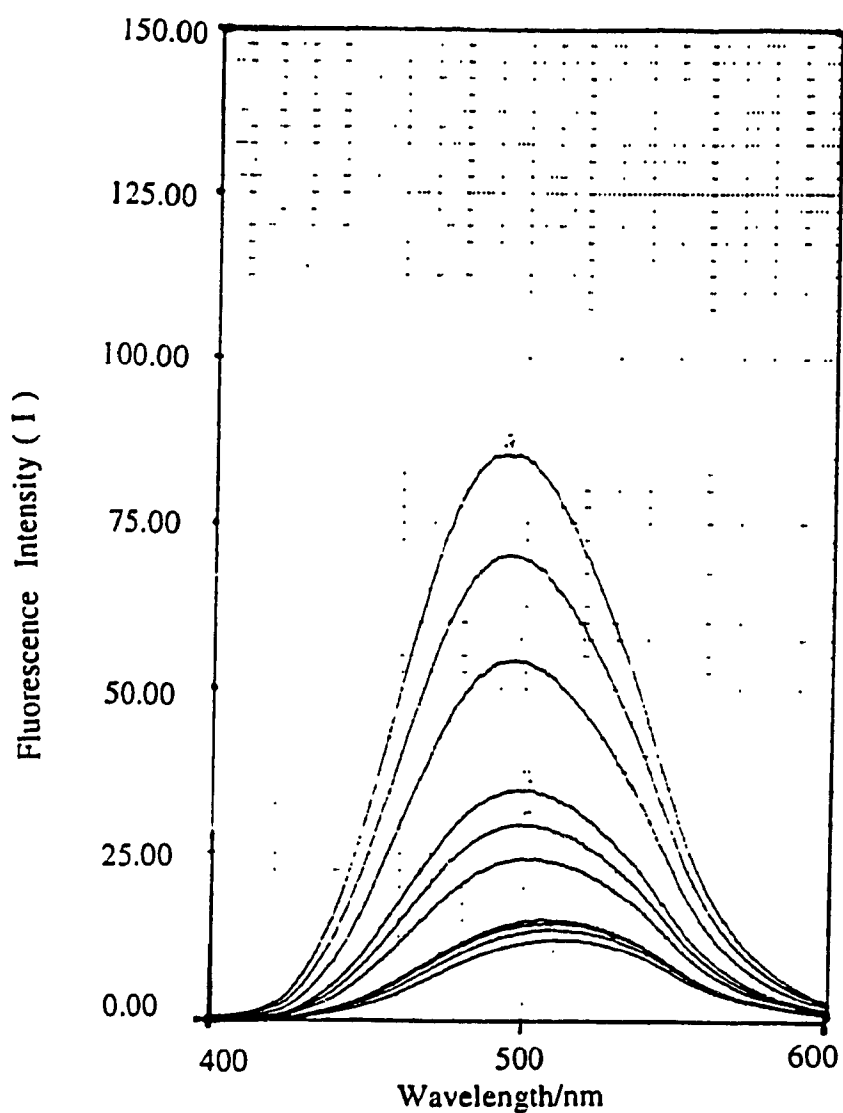


**Figure 2.3** Fluorescence emission spectra of  $1.00 \times 10^{-4}$  M ANS with an excitation wavelength of 368.0 nm in  $\alpha$ -CD. The concentrations of  $\alpha$ -CD (M) : 0.00,  $4.00 \times 10^{-4}$ ,  $8.00 \times 10^{-4}$ ,  $1.00 \times 10^{-3}$ ,  $4.80 \times 10^{-3}$ ,  $7.20 \times 10^{-3}$ ,  $9.60 \times 10^{-3}$ ,  $1.92 \times 10^{-2}$ ,  $2.88 \times 10^{-2}$ ,  $3.84 \times 10^{-2}$  from bottom to top. Excitation and emission band widths were 5.0 nm and 5.0 nm, respectively.

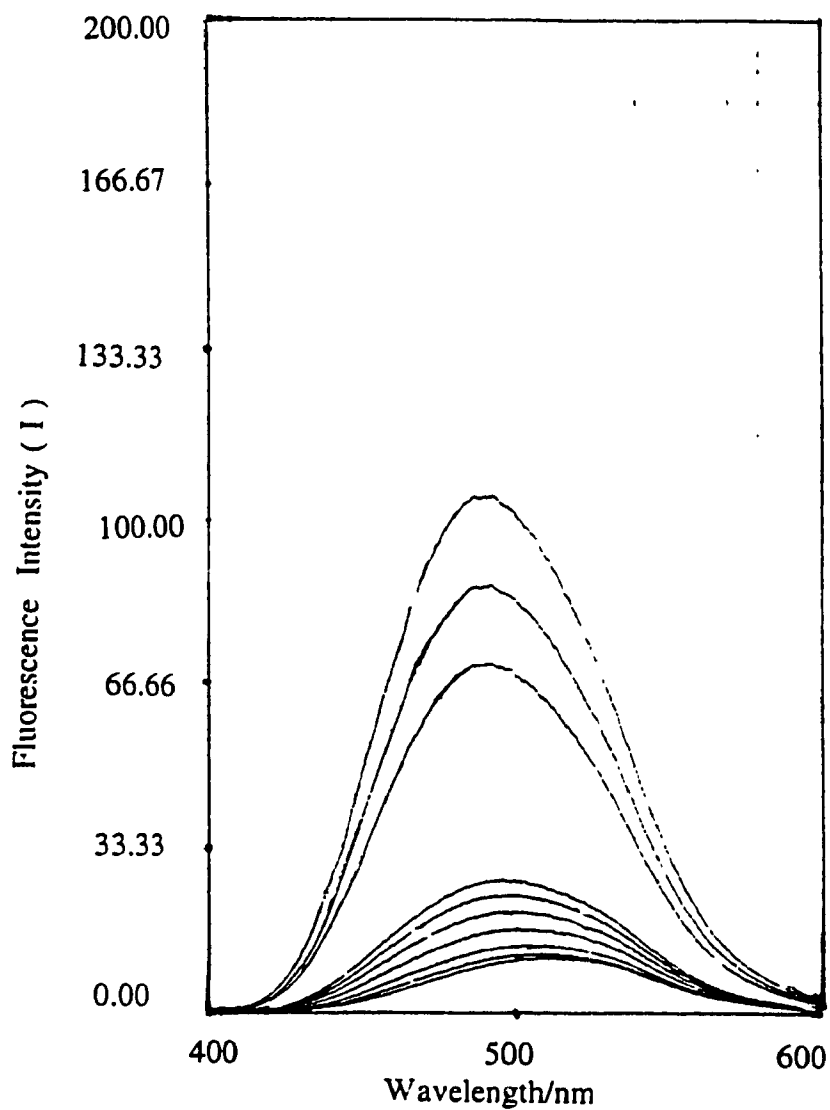


**Figure 2.4** Fluorescence emission spectra of  $1.00 \times 10^{-4}$  M ANS with an excitation wavelength of 368.0 nm in  $\beta$ -CD. The concentrations of  $\beta$ -CD (M): 0.00,  $1.00 \times 10^{-4}$ ,  $2.00 \times 10^{-4}$ ,  $4.00 \times 10^{-4}$ ,  $6.00 \times 10^{-4}$ ,  $8.00 \times 10^{-4}$ ,  $1.00 \times 10^{-3}$ ,  $4.00 \times 10^{-3}$ ,  $6.00 \times 10^{-3}$ ,  $8.00 \times 10^{-3}$  from bottom to top. Excitation and emission band widths were 5.0 nm and 5.0 nm, respectively.

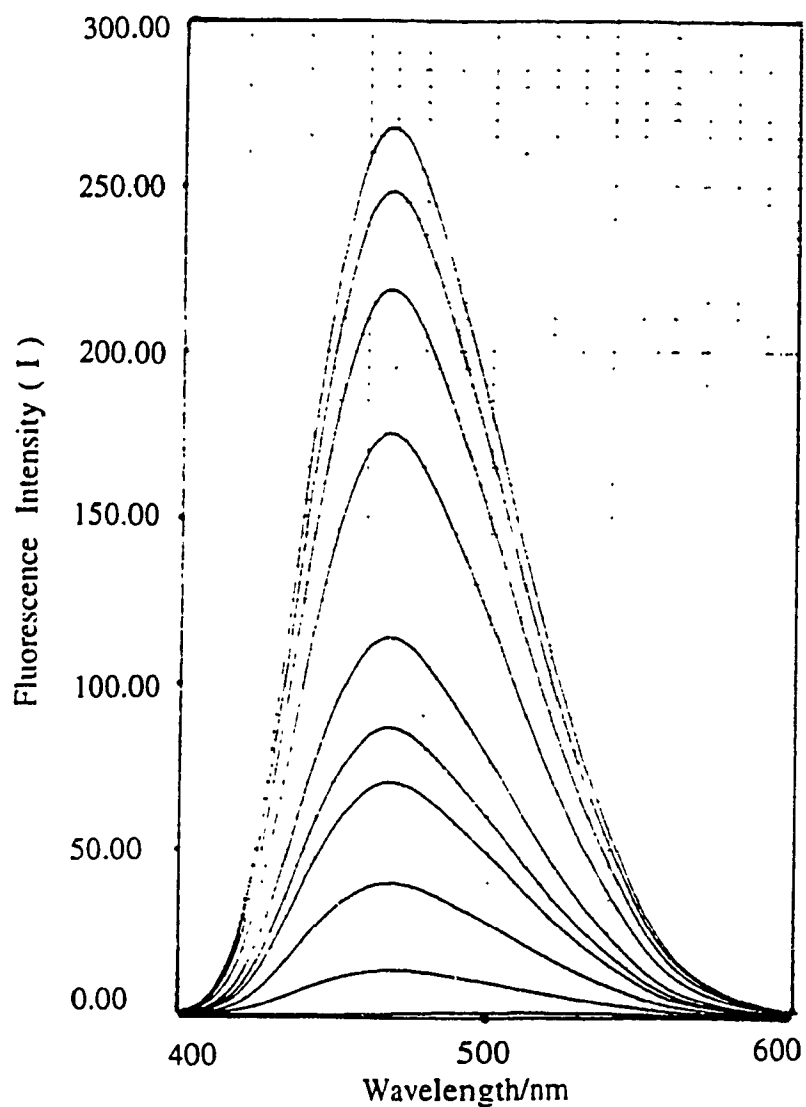


**Figure 2.5** Fluorescence emission spectra of  $1.00 \times 10^{-4}$  M ANS with an excitation wavelength of 368.0 nm in HP- $\beta$ -CD. The concentrations of HP- $\beta$ -CD (M): 0.00,  $1.00 \times 10^{-4}$ ,  $3.00 \times 10^{-4}$ ,  $6.00 \times 10^{-4}$ ,  $8.00 \times 10^{-4}$ ,  $1.20 \times 10^{-3}$ ,  $2.40 \times 10^{-3}$ ,  $4.00 \times 10^{-3}$ ,  $6.00 \times 10^{-3}$ ,  $8.00 \times 10^{-3}$  from bottom to top. Excitation and emission band widths were 1.5 nm and 3.0 nm, respectively.



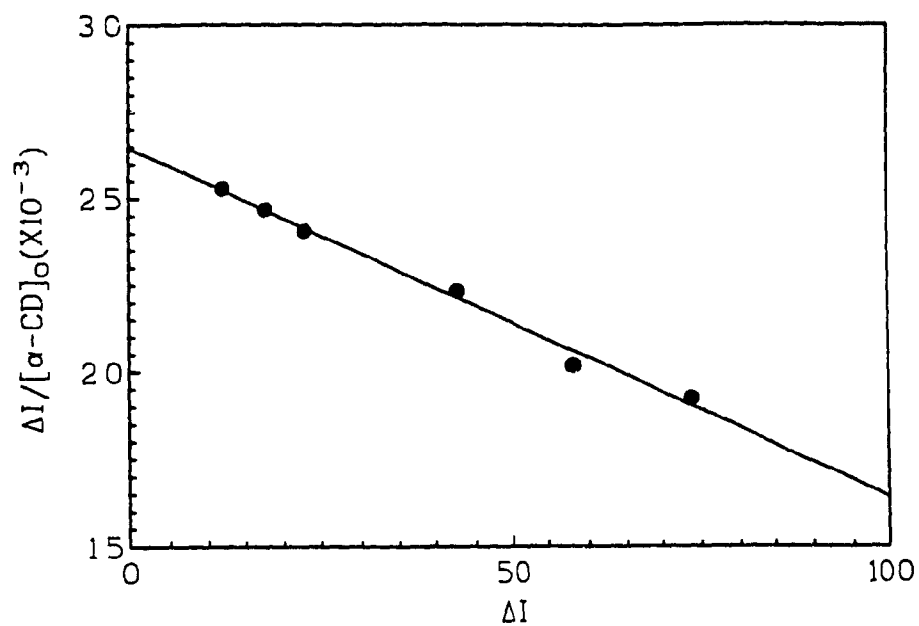


**Figure 2.6** Scatchard plot of ANS- $\alpha$ -CD at emission wavelength 494.4 nm.

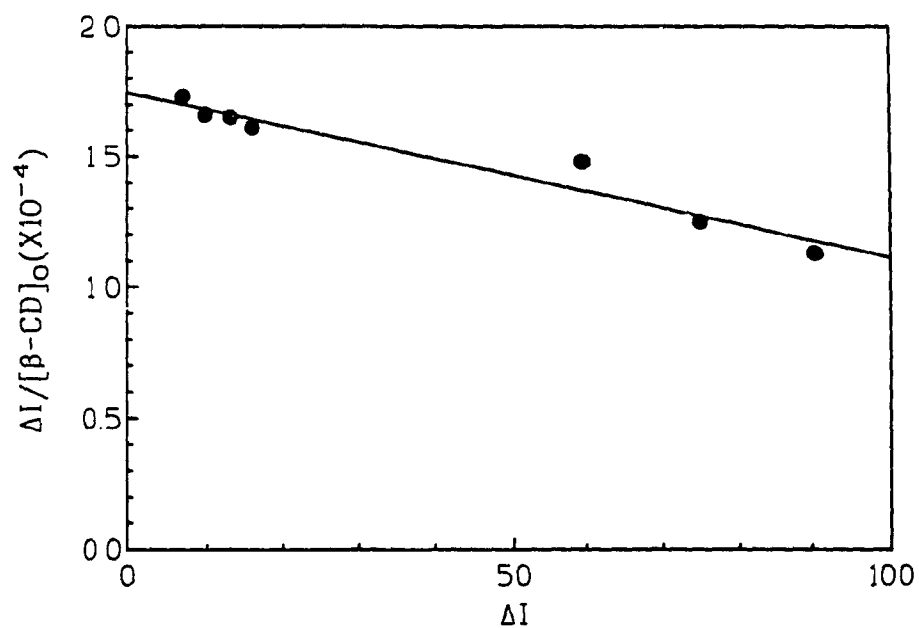


**Figure 2.7** Scatchard plot of ANS- $\beta$ -CD at emission wavelength 490.0 nm.

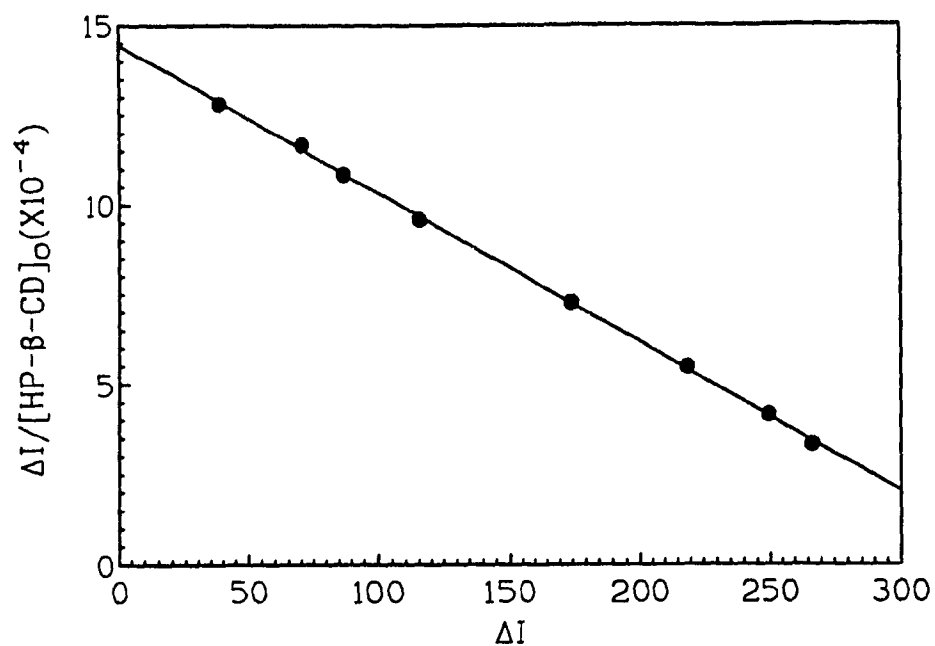


**Figure 2.8.** Scatchard plot of ANS-HP- $\beta$ -CD at emission wavelength 468.0 nm.

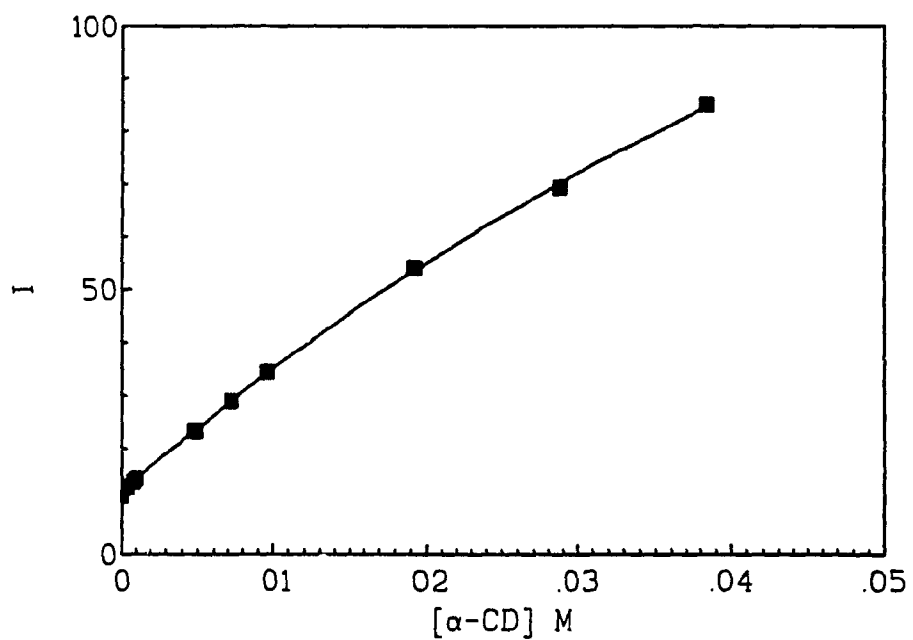


**Figure 2.9** Fluorescence intensity of  $1.00 \times 10^{-4}$  M ANS in  $\alpha$ -CD at emission wavelength 494.4 nm.

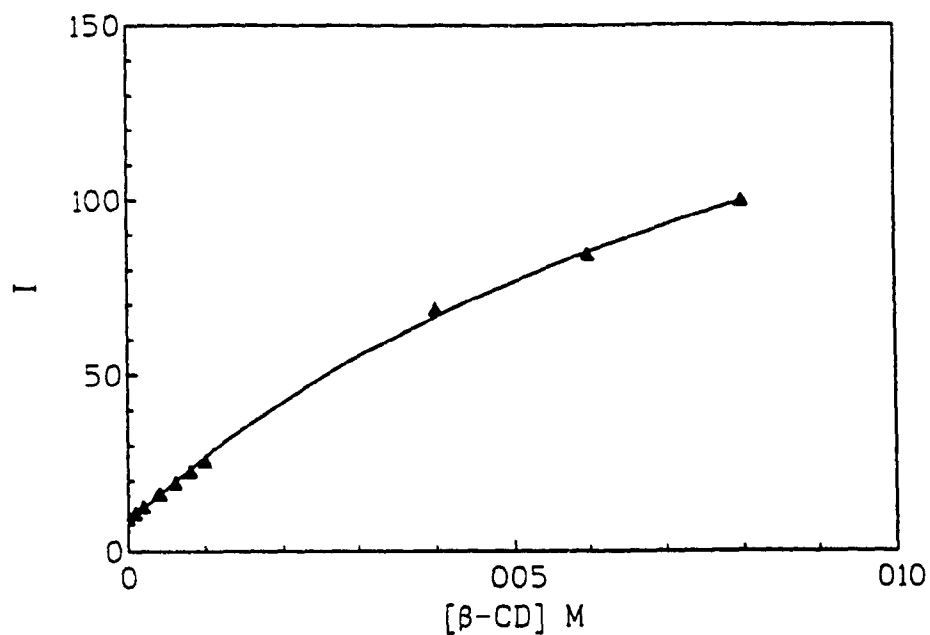


**Figure 2.10** Fluorescence intensity of  $1.00 \times 10^{-4}$  M ANS in  $\beta$ -CD at emission wavelength 490.0 nm.

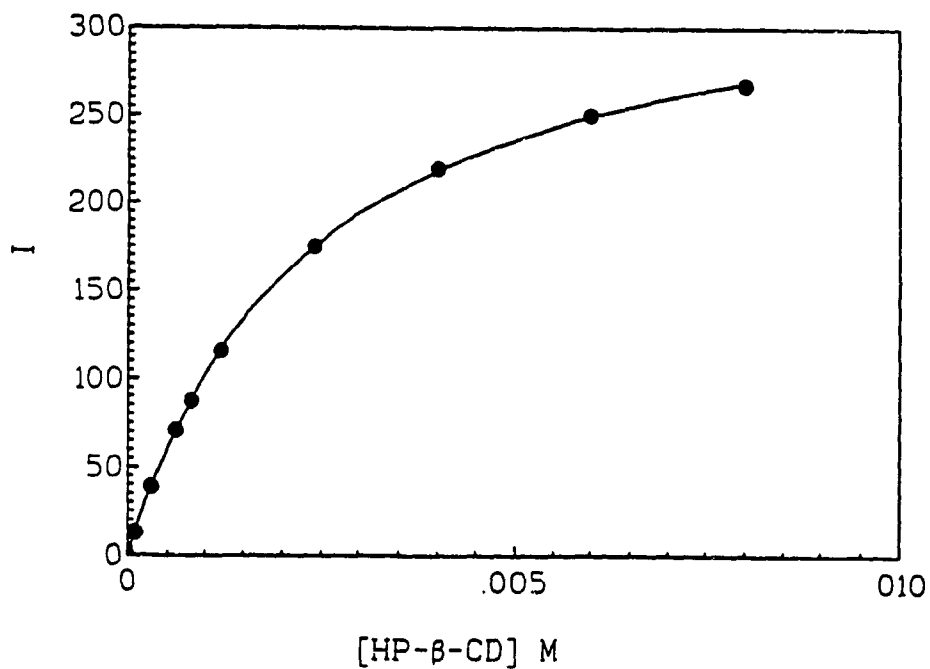


**Figure 2.11** Fluorescence intensity of  $1.00 \times 10^{-4}$  M ANS in HP- $\beta$ -CD at emission wavelength 468.0 nm.

CD,  $\beta$ -CD and HP- $\beta$ -CD, respectively. Appendix 4 contains the raw data for these fluorescence measurements. From the spectra we can see that emission intensity is very small in the absence of CD, but when the concentration of CD is increased, the fluorescence increases. When ANS is included in the CD cavity, its excited state is protected from quenching and non-radiative decay processes that readily occur in bulk aqueous solution, so the fluorescence of ANS is increased greatly relative to that observed in water alone<sup>1</sup>. At the same time, the emission wavelength shifts significantly towards the blue as the CD concentrations are increased. In the presence of excess CD, the emission wavelength and intensity are dominated by the CD-ANS complex. ANS exhibits a spectral shift of about 20 nm in the emission wavelength maximum in aqueous solution in the presence of excess  $\alpha$ -CD or  $\beta$ -CD, but a 44 nm blue-shift is observed with excess HP- $\beta$ -CD. The emission wavelengths for the complexes were used to record emission intensities ( $n = 3$ ) at various CD concentrations, and the linear and non-linear regression methods were used to evaluate association constants, assuming 1:1 ANS:CD binding.

Using the linear regression (Scatchard) method (Figure 2.6-2.8), association constants of  $10 \text{ M}^{-1}$ ,  $63 \text{ M}^{-1}$  and  $414 \text{ M}^{-1}$  for ANS inclusion complexes with  $\alpha$ -CD,  $\beta$ -CD and HP- $\beta$ -CD were obtained, respectively. For the same data, using the non-linear regression method (Figure 2.9-2.11) gave the association constants of  $9 \text{ M}^{-1}$ ,  $95 \text{ M}^{-1}$  and  $420 \text{ M}^{-1}$  for ANS complexation by with  $\alpha$ -CD,  $\beta$ -CD and HP- $\beta$ -CD, respectively. The difference in the  $\beta$ -CD values obtained by the two methods can be attributed to the relatively poor precision of the data as seen in Figure 2.7. A comparison of  $K_a$  values for the ANS-CD complexes is shown in Table 2.2. From these results we can see that

**Table 2.2.**  $K_a$  values of ANS-CD complexes

$K_a$ ( $M^{-1}$ )	ANS		
	$\alpha$ -CD	$\beta$ -CD	HP- $\beta$ -CD
Scatchard Plot	$10 \pm 1$	$63 \pm 7$	$414 \pm 4$
Regression method	$9 \pm 1$	$95 \pm 9$	$420 \pm 5$
Literature Values	$5^7, 2^7$	$110^4, 95^{14}, 77^{20}, 65^7, 64^{21}$	$585^{22}$

the association constants increase substantially from  $\alpha$ -CD to  $\beta$ -CD to HP-  $\beta$ -CD. For  $\alpha$ -CD,  $\beta$ -CD and HP- $\beta$ -CD, the association constants obtained in these experiments are reasonably similar to literature values<sup>4,7,14,20,21,22</sup>.

Binding between CDs and guests is dependent on both the size of the CD cavity and the size of the guest. Because the diameter of  $\alpha$ -CD is smaller than the diameter of  $\beta$ -CD, it has been suggested<sup>1</sup> that only the aniline part of the ANS molecule can be included in the  $\alpha$ -CD cavity, so the binding is weaker, and the association constant is smaller. Schneider and co-workers<sup>7</sup> used fluorescence and NMR techniques to study the mechanism of ANS inclusion in CDs and suggested that  $\beta$ -CD also prefers to include only the aniline group of ANS, instead of the naphthyl group, because binding is more effective if there is enough room for guest mobility within the cavity. The cavity sizes

thus explain the different ANS association constants for  $\alpha$ -CD and  $\beta$ -CD. It is interesting that ANS binding with HP- $\beta$ -CD is about 7 times stronger than with  $\beta$ -CD. Since  $\beta$ -CD and HP- $\beta$ -CD have almost the same internal diameter, there must be another factor influencing the binding. The only difference in structure is that there are hydroxypropyl groups on HP- $\beta$ -CD on the primary side of the cavity. The hydrophobicity of the modified  $\beta$ -CD cavity may be greater because of these groups, so that HP- $\beta$ -CD offers better protection than  $\beta$ -CD for ANS in the cavity, by shielding it from the surrounding aqueous environment. Effectively, the cavity diameters are the same, but the depths are different. These results are similar to those observed in the binding of naphthalene included with  $\beta$ -CD and HP- $\beta$ -CD<sup>23</sup>, where the enhanced fluorescence with HP- $\beta$ -CD was attributed to a more hydrophobic cavity.

The blue-shifts of the ANS emission wavelength are also an indicator of changes in the hydrophobicity of the environment surrounding ANS. The greater the blue-shift, the greater is the hydrophobicity experienced by ANS inside the cavity. The 44 nm blue-shift observed with HP- $\beta$ -CD indicates much greater hydrophobicity than the 20 nm blue-shift observed with  $\alpha$ -CD and  $\beta$ -CD.

The association constants determined here will be used for the next work, involving the displacement of ANS by spectroscopically invisible guests.

The effect of pH on the fluorescence intensity of ANS solutions in water,  $\beta$ -CD and HP- $\beta$ -CD have been studied (Appendix 5) and no effect was observed over pH 3.9-7.9. So it is suggested that the association constant is not affected significantly by the pH under the experimental conditions, and it is not necessary to use a buffer in most

experiments.

### 2.3.3 Association of 2-Propanol and t-Butanol with $\beta$ -CD and HP- $\beta$ -CD

Figures 2.12-2.15 show the spectra of ANS-CD solutions as a function of added alcohol concentration. Raw data for these experiments are given in Appendix 6. In these experiments, a decrease in fluorescence intensity is observed when alcohol is added to a solution containing fixed CD and ANS concentrations.

ANS and alcohols compete for the CD cavity. Alcohol displaces ANS from the CD interior, resulting in decreased fluorescence intensity. In determining association constants we have assumed that CD reacts with alcohol in a 1:1 molar ratio. An equation has been obtained to evaluate the association constants (eq. 4, Appendix 3). Plots of  $1/\Delta I$  versus  $1/[\text{propanol}]$  or  $1/[\text{t-butanol}]$  were obtained for  $\beta$ -CD and HP- $\beta$ -CD (Figure 2.16-2.19). From the slopes and intercepts of these plots the dissociation constants for  $\beta$ -CD-propanol, HP- $\beta$ -CD-propanol,  $\beta$ -CD-t-butanol and HP- $\beta$ -CD-t-butanol are calculated as 0.163 M, 1.25 M, 0.022 M and 0.49 M, respectively, by using equation 5. From the reciprocal of the dissociation constants, the association constants are obtained as  $6.1 \pm 1.0 \text{ M}^{-1}$ ,  $0.80 \pm 0.4 \text{ M}^{-1}$ ,  $45.6 \pm 0.8 \text{ M}^{-1}$  and  $2.0 \pm 0.1 \text{ M}^{-1}$  for  $\beta$ -CD-propanol, HP- $\beta$ -CD-propanol,  $\beta$ -CD-t-butanol and HP- $\beta$ -CD-t-butanol, respectively. Table 2.3 shows a comparison of values obtained in these experiments with literature values, obtained by other methods<sup>5,15</sup>.

From these results, it can be seen that the association constants for alcohols with  $\beta$ -CD are larger than those with HP- $\beta$ -CD. This indicates that there are differences of binding the alcohols between these two cyclodextrins. In HP- $\beta$ -CD most of the primary

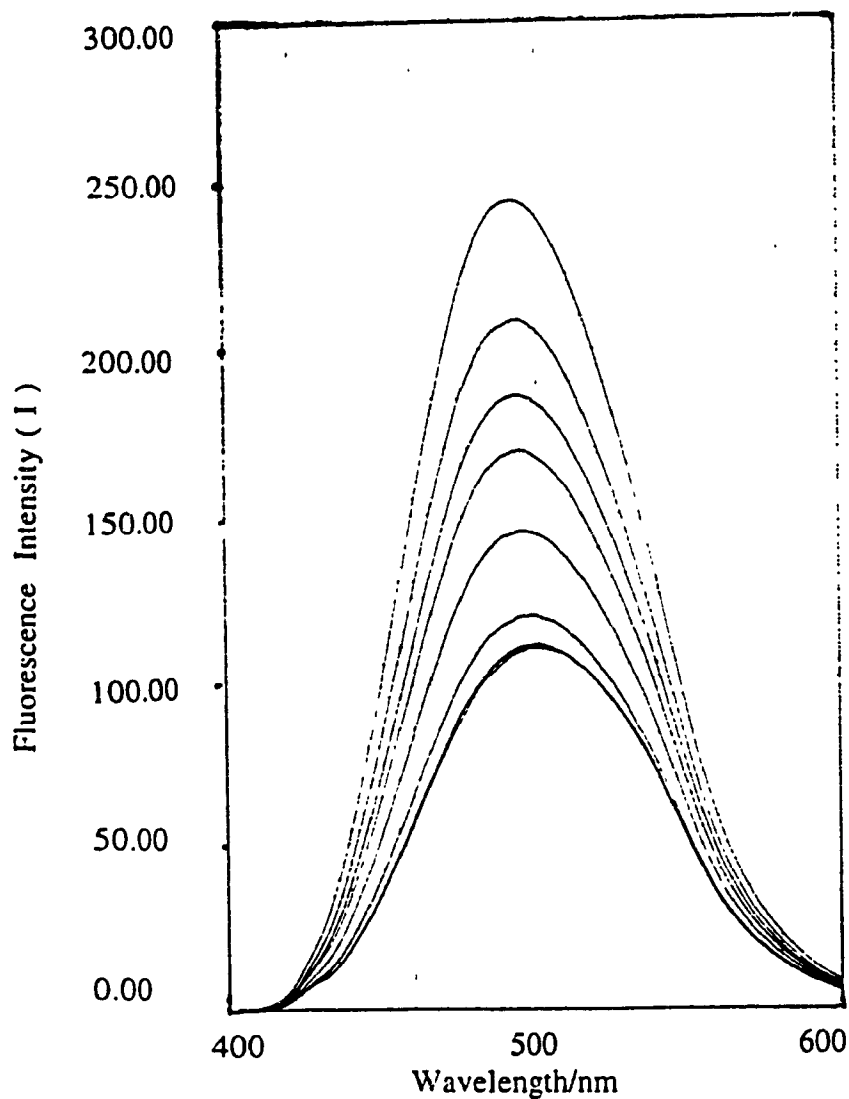


**Figure 2.12** Fluorescence emission spectra of  $1.00 \times 10^{-4}$  M ANS +  $4.20 \times 10^{-3}$  M  $\beta$ -CD. The concentrations of 2-propanol (M): 0.000, 0.0624, 0.125, 0.187, 0.312, 0.624, 0.936, 1.144 from top to bottom.  $\lambda_{\text{ex}} = 368.0$  nm. 0.01 M acetate buffer pH = 5.3. Excitation and emission band widths were 5.0 nm and 3.0 nm, respectively.



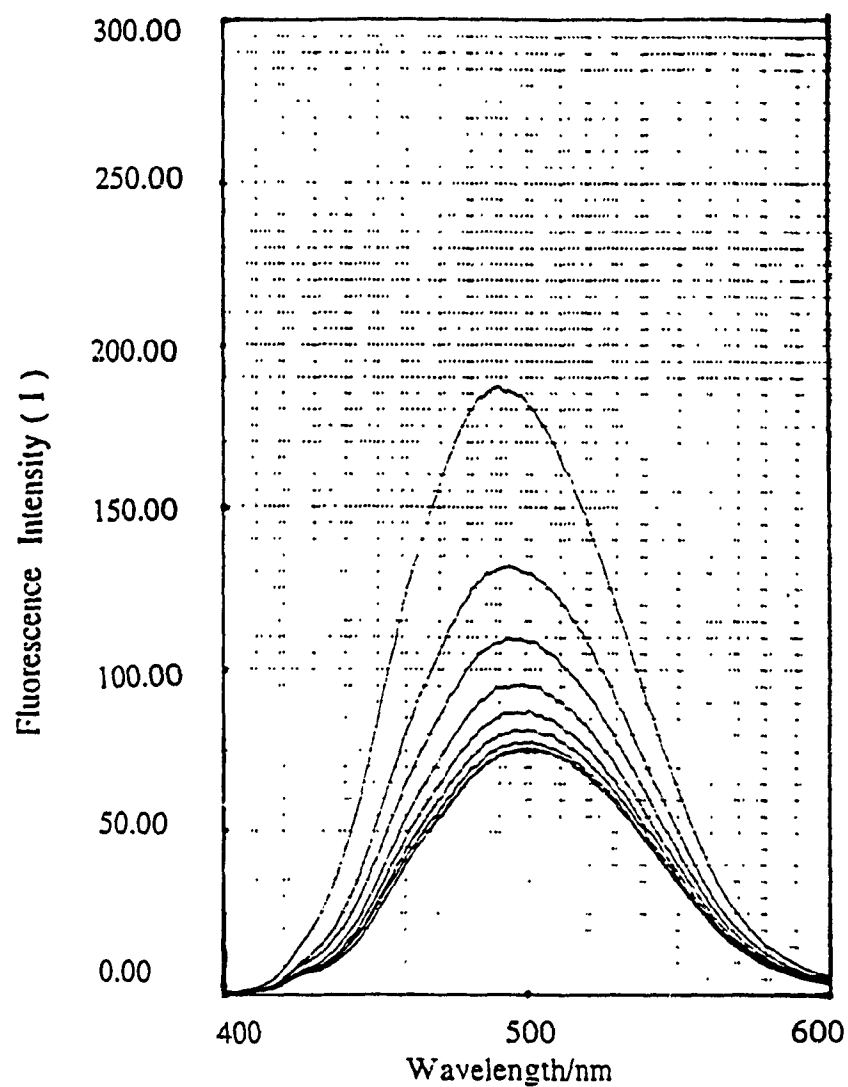


**Figure 2.13** Fluorescence emission spectra of  $1.00 \times 10^{-4}\text{M}$  ANS +  $4.20 \times 10^{-3}\text{M}$   $\beta$ -CD. The concentrations of t-butanol (M): 0.000, 0.020, 0.040, 0.060, 0.080, 0.100, 0.120, 0.130, 0.140 from top to bottom.  $\lambda_{\text{ex}} = 368.0$  nm. Excitation and emission band widths were 5.0 nm and 3.0 nm, respectively.

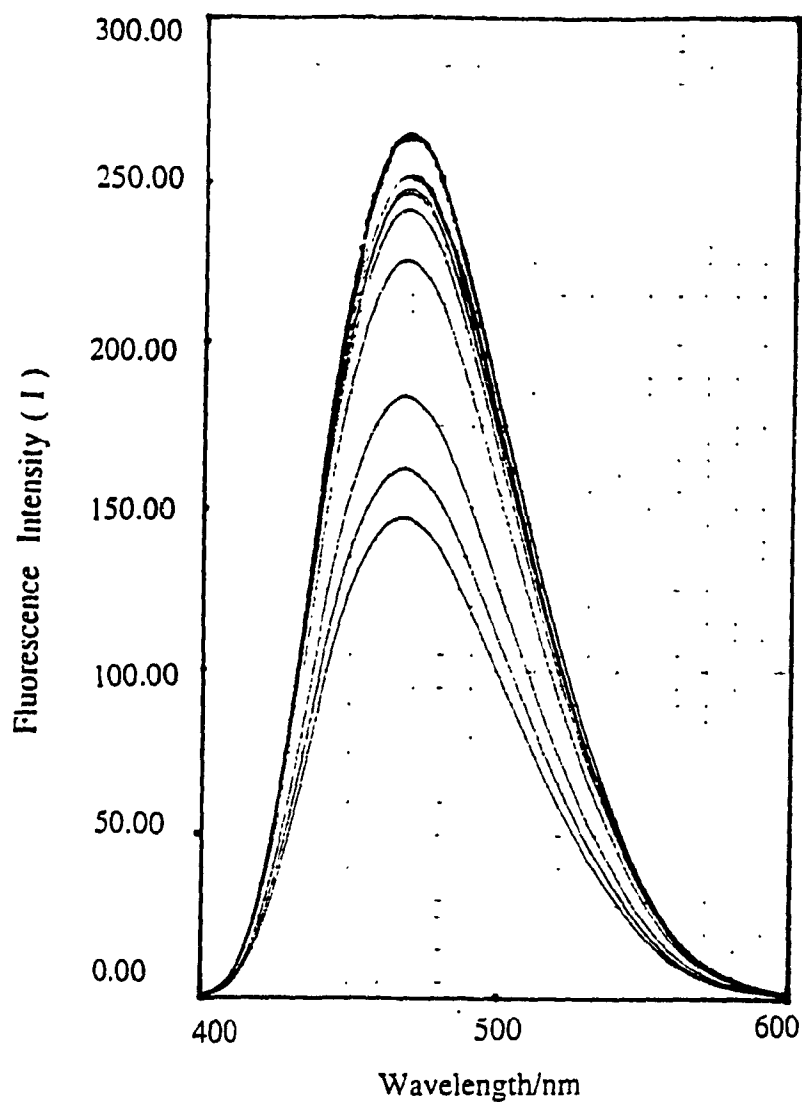


**Figure 2.14** Fluorescence emission spectra of  $1.00 \times 10^{-4}$  M ANS +  $8.00 \times 10^{-3}$  M HP- $\beta$ -CD. The concentrations of 2-propanol (M): 0.000, 0.125, 0.146, 0.166, 0.187, 0.312, 0.624, 0.832, 1.040 from top to bottom.  $\lambda_{ex} = 368.0$  nm. 0.01 M acetate buffer pH = 5.3. Excitation and emission band widths were 1.5 nm and 3.0 nm, respectively.

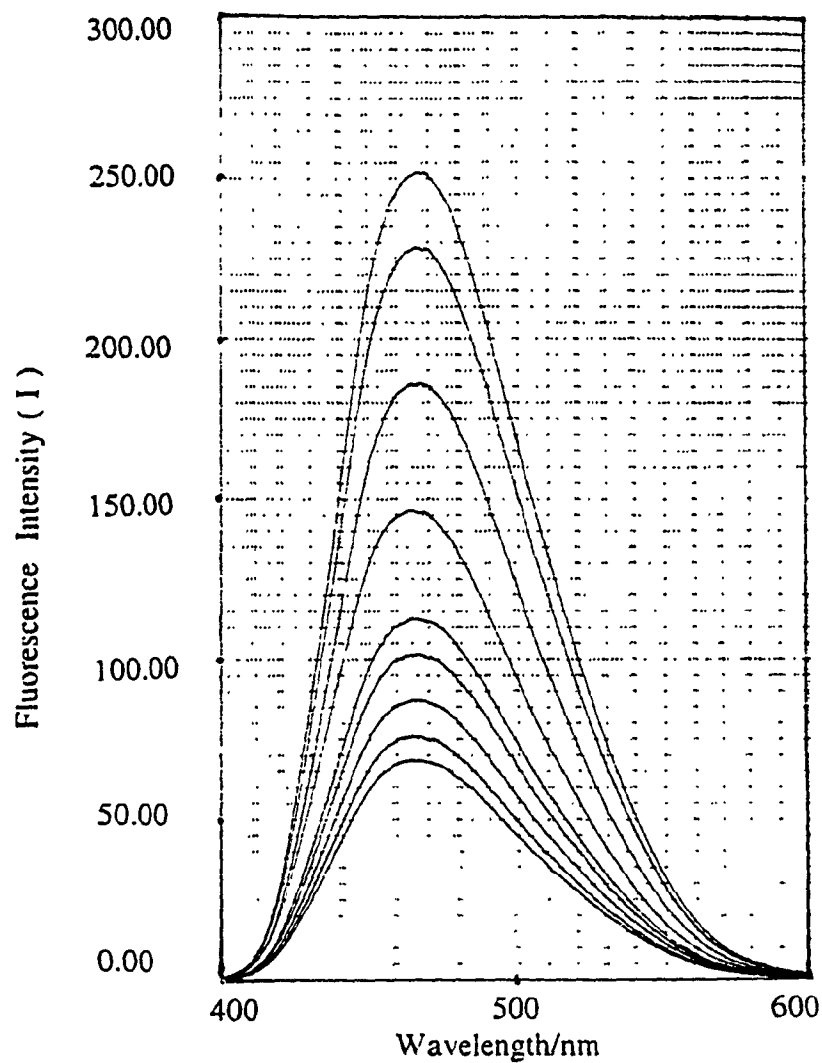


**Figure 2.15** Fluorescence emission spectra of  $1.00 \times 10^{-4}$  M ANS +  $8.00 \times 10^{-3}$  M  $\beta$ -CD. The concentrations of t-butanol (M): 0.000, 0.050, 0.150, 0.250, 0.400, 0.500, 0.600, 0.700, 0.800 from top to bottom.  $\lambda_{ex} = 368.0$  nm. Excitation and emission band widths were 1.5 nm and 3.0 nm, respectively.

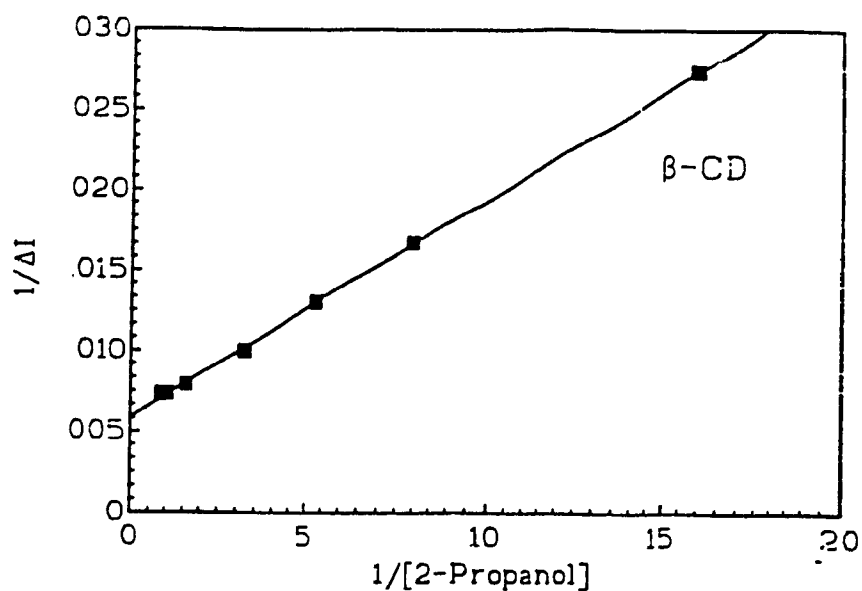


**Figure 2.16** Double reciprocal plot of  $\Delta I$  and [2-propanol] for ANS- $\beta$ -CD, according to equation 4.

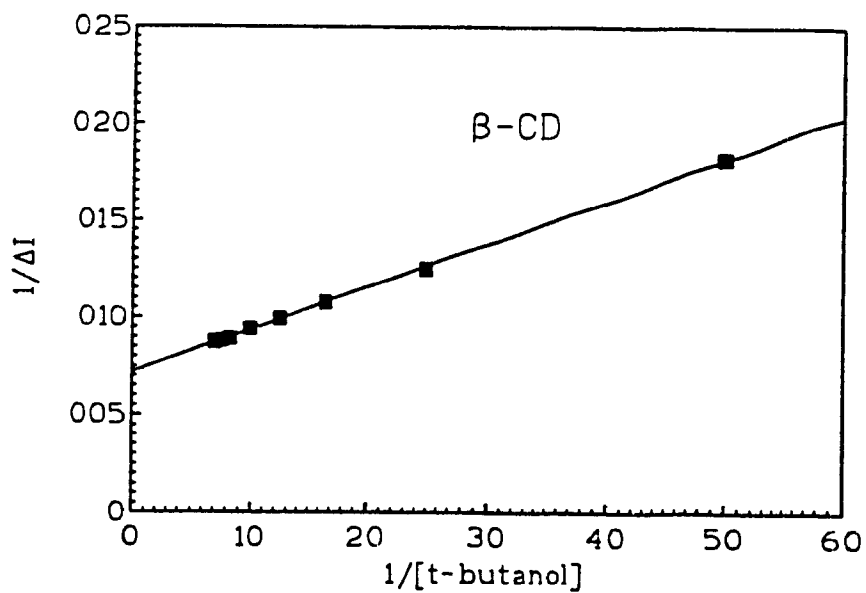


**Figure 2.17** Double reciprocal plot of  $\Delta I$  and [t-butanol] for ANS- $\beta$ -CD, according to equation 4.

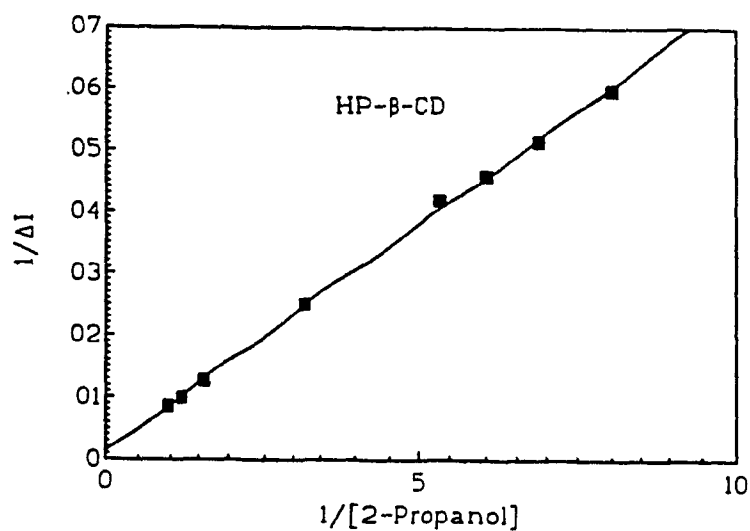


**Figure 2.18** Double reciprocal plot of  $\Delta I$  and  $[2\text{-propanol}]$  for ANS-HP- $\beta$ -CD, according to equation 4.

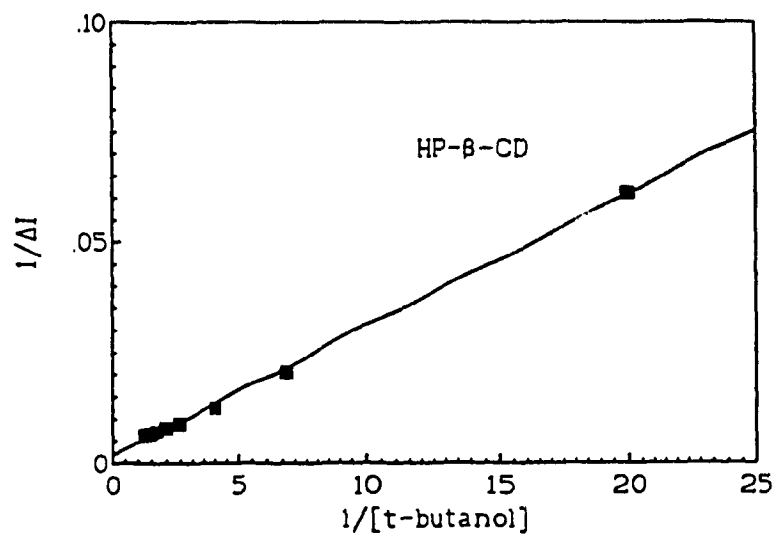


**Figure 2.19** Double reciprocal plot of  $\Delta I$  and  $[t\text{-butanol}]$  for ANS-HP- $\beta$ -CD, according to equation 4.

**Table 2.3**  $K_a$  Values for CD - Alcohol Complexes

Host	Guest	$K_a$ ( $M^{-1}$ )	Literature Value ( $M^{-1}$ )
$\beta$ -CD	2-Propanol	$6.1 \pm 1.0$	$3.8^{15}$
	t - Butanol	$45.6 \pm 0.8$	$47.9^{15}$
HP- $\beta$ -CD	2-Propanol	$0.8 \pm 0.4$	$3.6^5$
	t - Butanol	$2.0 \pm 0.1$	$25^5$

hydroxyl groups of  $\beta$ -CD are derivatized with 2-hydroxypropyl groups, and these may hinder the entry of the alcohol into the cavity. The data also show that association constants for both CDs with 2-propanol are smaller than those with t-butanol. This may be because t-butanol is more hydrophobic than 2-propanol, or because the bulky t-butanol fits the CD cavity better. Association constants found for  $\beta$ -CD-alcohol complexes agree with literature values, but the values obtained for HP- $\beta$ -CD-alcohol complexes show a big discrepancy, and are about one order of magnitude lower than the literature values. The literature values were determined by an inhibition kinetics method<sup>5</sup>. This method is also an indirect method, where formation of ternary complexes was not considered. In this method, alcohol is added at various concentrations to a solution of the m-nitrophenyl acetate and CD, and its effect on the rate of cleavage of the ester is monitored through the absorbance of the product. The reaction, and alcohol binding, occurs under very basic conditions (pH = 11.6). In addition to alcohol binding, there may be other factors affecting the rate of m-nitrophenyl acetate hydrolysis at pH 11.6, or the fluorescence

emission of ANS at pH 4-5, when alcohol is added to the probe-CD mixture. It may be possible that alcohol binding to the hydroxypropyl groups on the periphery of the HP- $\beta$ -CD cavity, without displacing ANS completely from the cavity, is undetected in the fluorescence method.

Warner and co-workers<sup>24-25</sup> studied the influence of alcohols on the fluorescence of pyrene in solutions containing  $\beta$ -CD and  $\gamma$ -CD and found the environment surrounding the pyrene was less polar when various alcohols were added. Both the fluorescence lifetimes and formation constants were enhanced in the presence of alcohols. Warner suggested that ternary complexes were formed, and that alcohols may be positioned in the open end of the CD torus and/or extended into the cavity as a "space regulator", eliminating some ordered water and reducing the degree of fluorophore-water interaction, enhancing the hydrophobic character of the  $\beta$ -CD interior or facilitating the association of CDs and pyrene. According to Warner's work it is suggested that two mechanisms could be involved in the binding of alcohol in the HP- $\beta$ -CD-ANS system. One is the formation of a ternary complex with the alcohol molecule positioned on the rim of the cavity, that would be expected to increase the fluorescence of the CD-ANS complex, while the second involves displacement of ANS from the CD cavity by the alcohol, resulting in decreased fluorescence. In these experiments, it is evident that the displacement mechanism is dominant.

## 2.4 References

- (1) Cramer, F.; Saenger, W.; Spatz, H.-Ch. *J. Am. Chem. Soc.*, **1967**, 89, 14-20.
- (2) Aoyama, Y.; Nagai, Yoshiro.; Otsuki, J-I.; Kobayashi, K.; Toi, H. *Tetrahedron Letters*. **1992**, 33, 3775-3778.
- (3) Kondo, H.; Nakatani, H.; Hiromi, K. *J. Biochem.*, **1976**, 79, 393-405.
- (4) Catena , G. C.; Bright, F.V. *Anal. Chem.*, **1989**, 61, 905-909.
- (5) Tee. O.S.; Gadosy, T.A.; Giorgi, J.B. *J. Chem. Soc. Perkin Trans. 2*, **1993**, 1705-1706.
- (6) Lavandier, C.D.; Pelletier, M.P.; Reinsborough, V.C. *Aust. J. Chem.*, **1991**, 44, 457-461.
- (7) Schneider, H-J.; Blatter, T.; Simova, S. *J. Am. Chem. Soc.*, **1991**, 113, 1996-2000.
- (8) Uekama, K.; Hirayama, F.; Nasu, S.; Matsuo, N.; Irie, T. *Chem.Pharm.Bull.*, **1978**, 26, 3477-3484.
- (9) Anigbogu, V.C.; Muñoz de la Peña, A.; Ndou, T.T.; Warner, I.M. *Anal. Chem.*, **1992**, 64, 484-489.
- (10) Fujimura, K.; Ueda, T.; Kitagawa, M.; Takayanagi, H.; Ando, T. *Anal. Chem.*, **1986**, 58, 2668-2674.
- (11) Husain, N.; Anigbogu, V.C.; Cohen, M.R.; Warner, I.M. *J. Chromatogr.*, **1993**, 635, 211-219.
- (12) Connors, K.A. *Binding Constants: a measurement of molecular complex stability*; John Wiley & Sons: New York, **1987**. pp 339 - 355
- (13) Selvidge, L.A.; Eftink, M.R. *Anal. Biochem.*, **1986**, 154, 400-408.



- (14) Aoyama, Y.; Nagai, Yoshiro.; Otsuki, J-I.; Kobayashi, K.; Toi, H. *Angew. Chem. Int. Ed. Engl.*, **1992**, 31, 745-747.
- (15) Matsui, Y; Mochida, K. *Bull. Chem. Soc. Jpn.*, **1979**, 52, 2808- 2814.
- (16) Pendergast, D.D.; Connors, K.A.. *J. Pharm. Sci.*, **1984**, 73, 1779-1783.
- (17) Harada, A.; Nozakura, S.; *Polym. Bull. (Berlin)*, **1982**, 8, 141.
- (18) Gadosy, T.A.; Tee, O.S. *J. Chem. Soc. Perkin Trans. 2.*, **1994**, 715-721.
- (19) Tee, O.S.; Du, X-X. *J. Am. Chem. Soc.*, **1992**, 114, 620-629.
- (20) Tabushi, I.; Shimizu, N.; Sugimoto, T.; Shiozuka, M.; Yamamura, K. *J. Am. Chem. Soc.*, **1977**, 99, 7100-7102.
- (21) Franke, J.; Merz, F.; Lorensky, H. W.; Muller, W. M.; Werner, W.; Vögtle, F.; *J. Inclusion Phenom.*, **1985**, 3, 471 - 478.
- (22) Tee, O.S.; Gadosy, T.A.; Giorgi, J.B. Submit to *Can. J. Chem.*, (1995)
- (23) Zung, J.B.; Ndou, T.T.; Warner, I.M. *Applied Spectroscopy*, **1990**, 44, 1491-1493.
- (24) Zung, J.B.; Muñoz de la Peña, A.; Ndou, T.T.; Warner, I.M. *J. Phys. Chem.* **1991**, 95, 6701-6706.
- (25) Muñoz de la Peña, A.; Ndou, T.T.; Zung, J.B.; Greene, K.L.; Live, D.H.; Warner, I.M. *J. Am. Chem. Soc.*, **1991**, 113, 1572-1577.

### 3.1 Introduction

The diagram illustrates the chemical equilibrium between the stationary phase (left) and the mobile phase (right), separated by a vertical dashed line. In the stationary phase, the species are  $[G]_s$  and  $[CD-G]_s$ . In the mobile phase, the species are  $[G]_m$ ,  $[CD]_m$ , and  $[CD-G]_m$ . A horizontal double-headed arrow connects  $[G]_s$  and  $[G]_m$ . A vertical double-headed arrow connects  $[CD]_m$  and  $[CD-G]_m$ . A horizontal double-headed arrow also connects  $[CD-G]_s$  and  $[CD-G]_m$ .

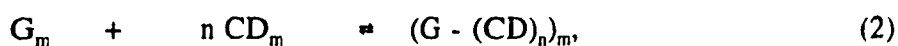
45

HPLC has been used to determine the association constants of CD-guest inclusion complexes, based on changes in the retention of the guest when the mobile phase CD concentration is varied. Early work in this area applied the model shown above in Scheme 1.<sup>4</sup> CD is present as a mobile-phase additive, and its interaction with the stationary phase, a strong ion-exchange resin, is assumed negligible. With this model, the observed retention time of the guest ( $t_{r,obs}$ ) at a given mobile phase CD concentration ( $[CD]_m$ ) is related to the CD-guest association constant,  $K$ , by equation 1, below:

$$\frac{[CD]_m}{(t_{r,0} - t_{r,obs})} = \frac{[CD]_m}{(t_{r,0} - t_{r,c})} + \frac{1}{K(t_{r,0} - t_{r,c})}, \quad (1)$$

where  $t_{r,0}$  and  $t_{r,c}$  are the limiting retention times of free and CD-bound guest, respectively. The value of  $K$  is obtained from a plot of the left hand term of eq. 1 against  $[CD]_m$ , as the slope:y-intercept. This method was applied to a range of guests, including barbiturates, phenothiazines, sulfonamides and sulfonylureas,<sup>4</sup> and the results correlated well ( $R = 0.998$ ) with values obtained by UV-visible spectroscopy. All of these guests were known, or assumed, to associate with CDs to form 1:1 complexes.

In 1990, Mohseni and Hurtubise<sup>5</sup> extended this method to allow the determination of association constants for the general reaction



where the subscript m again refers to the mobile phase, and n is a stoichiometric coefficient that would, for example, have a value of 1/2, or 2 for 2:1 or 1:2 guest:CD stoichiometry, respectively.

In these experiments, a C<sub>18</sub> reversed-phase stationary phase was used, and guest retention times were monitored as a function of mobile-phase CD concentration. Observed capacity factors,  $k' = (t_r - t_0)/t_0$ , were related to the formation constant K by equation 3, below:

$$1/k' = 1/k'_0 ( 1 + K [ CD ]_M^n ), \quad (3)$$

where  $k'_0$  is the capacity factor of the guest in the absence of CD. Plots of  $1/k'$  against  $[CD]_M^n$  are linear for a correctly-chosen n value, and K is determined from the ratio of slope to y-intercept ratio. Anigbogu et al.<sup>6</sup> recently used this method to show that pyrene forms a 2:1 complex with  $\beta$ -CD.

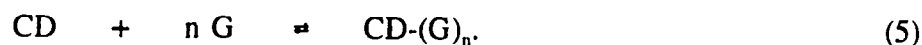
With these methods, the retention time of the guest is observed to decrease as the mobile-phase concentration of CD is increased. In all cases, uncomplexed CD was assumed not to interact with the stationary phase, so that only the guest and guest-CD complex were retained. Until recently, CDs were believed not to be retained on reversed-phase columns because of their hydrophilic exterior, but recent studies have shown<sup>7</sup> that CDs are retained on the reversed-phase columns at low mobile phase concentrations of methanol, over the 3%-7% range. The capacity factors of CDs were found to decrease when the mobile-phase concentration of methanol was increased. In this work, Koizumi



of CD concentration distribution used in this work. In our model, free CD is retained on the stationary phase, while the guest:CD complex is not retained. Under these conditions, it can be shown (Appendix 7) that the observed capacity factor for CD,  $k'$ , is related to the mobile phase guest concentration,  $[G]_m$ , by equation 4, below:

$$1/k' = 1/k'_0 ( 1 + K [ G ]_m^n ), \quad (4)$$

where  $k'_0$  is the CD capacity factor in the absence of guest, and  $K$  is the association constant for the reaction



Because CDs do not produce a detectable absorbance or fluorescence signal, 1-anilino-8-naphthalenesulfonic acid (ANS) was used as a probe, present in the mobile phase at low concentration, to allow fluorescence detection of eluting CDs. The first part of this chapter describes the optimization of this detection method. The second part of this chapter involves the development of the method to determine the association constants of CD-guest complexes,  $K$ , and the complexation stoichiometries,  $1:n$ , of CD:alcohol by RP-HPLC, where CD is the injected sample, and the guest is the mobile phase modifier. Results obtained by this new method are compared with an accepted method, spectroscopic displacement (chapter 2), using the representative guests, 2-propanol and t-butanol.

## **3.2 Experimental**

### **3.2.1 Reagents**

2-Propanol (HPLC grade) was purchased from Sigma-Aldrich. t-Butanol and ANS were obtained from Aldrich.  $\beta$ -CD and HP- $\beta$ -CD ( $MW_{avg} = 1500$ , D.S = 0.8) were obtained from Aldrich in the 2-propanol experiments, and were from Wacker (Pharmaceutical grade, for HP- $\beta$ -CD  $MW_{avg} = 1560$ , D.S = 0.9) in the t-butanol experiments. Nanopure water (Barnstead) was used to prepare all solutions. All reagents were used as received.

### **3.2.2 Apparatus**

The HPLC system consisted of a LKB 2249 LC pump, a sample injector (100 $\mu$ l sample loop), and a Hewlett Packard 1046A fluorescence detector that was set at excitation and emission wavelengths of 368.0 nm and 490.0 nm for  $\beta$ -CD, and 368.0 nm and 468.0 nm for HP- $\beta$ -CD, respectively. For most experiments the column used was an Econosphere C<sub>18</sub> (5 $\mu$ m, 0.46 x 25 cm) purchased from Alltech. In one case, a reversed-phase inertsil phenyl column (Meta Chem, 5  $\mu$ m, 0.3 x 10 cm) was used.

### **3.2.3 Methods**

#### **3.2.3.1 Flow Injection**

As described in Chapter 2, the fluorescence of ANS increases upon binding to CDs, so ANS can act as a probe to detect eluting CDs. In order to find the best ANS concentration for detection, a series of experiments were arranged using the HPLC equipment in a flow injection analysis system, that is, without a column. Solutions of ANS in water were used as the mobile phase, and solutions of  $\beta$ -CD in mobile phase

were injected. The background fluorescence of the mobile phase, and the peak fluorescence caused by the injected  $\beta$ -CD, were measured.

### 3.2.3.2 Reversed Phase HPLC

Mobile phases were prepared by adding 50.0 ml of a  $1.00 \times 10^{-3}$  M ANS stock solution and different volumes of pure modifier to a 500 ml volumetric flask, and diluting to the mark with nanopure water. Mobile phases with different concentrations of the modifiers 2-propanol or t-butanol, and the same concentration of ANS ( $1.00 \times 10^{-4}$  M) were prepared in this way.

The mobile phase was filtered through a  $0.2 \mu\text{m}$  nylon membrane filters (Gelman) and degassed under vacuum before use. The mobile phase flow rate was 1.0 ml/min, and the column was conditioned for about one hour with a new mobile phase prior to injection. Injected solutions contained  $5.00 \times 10^{-3}$  M  $\beta$ -CD or HP- $\beta$ -CD solutions, and were prepared by weighing 0.0567 g  $\beta$ -CD or 0.075 g HP- $\beta$ -CD into a 10.0 ml volumetric flask, and diluting to the mark with mobile phase. Three injections of each of CD and nanopure water were made for each mobile phase. The negative peak observed for water elution was used to determine void volume ( $t_0$ ). Average  $t_r$  and  $t_0$  values were calculated at each mobile phase modifier concentration and capacity factors,  $k'$  ( $(t_r - t_0)/t_0$ ) were then calculated. Plots of  $1/k'$  against  $[G]^n$  were then constructed according to equation 4, and the minimum  $n$  value yielding a linear plot, within experimental error, was used for the calculation of  $K$ .

## 3.3 Results and Discussion

### *Optimization of ANS concentration*



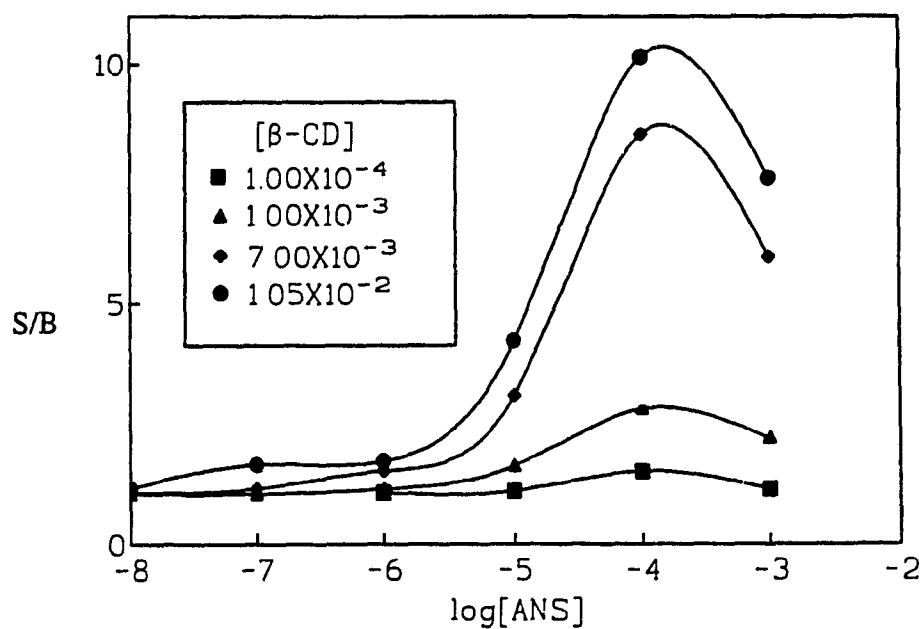


**Figure 3.1** Signal-to-background ratio (S/B) vs log [ANS] for different injected  $\beta$ -CD concentrations. Excitation and emission wavelengths were 368.0 nm and 490.0 nm, respectively, and the mobile phase flow rate was 1.0 ml/min.

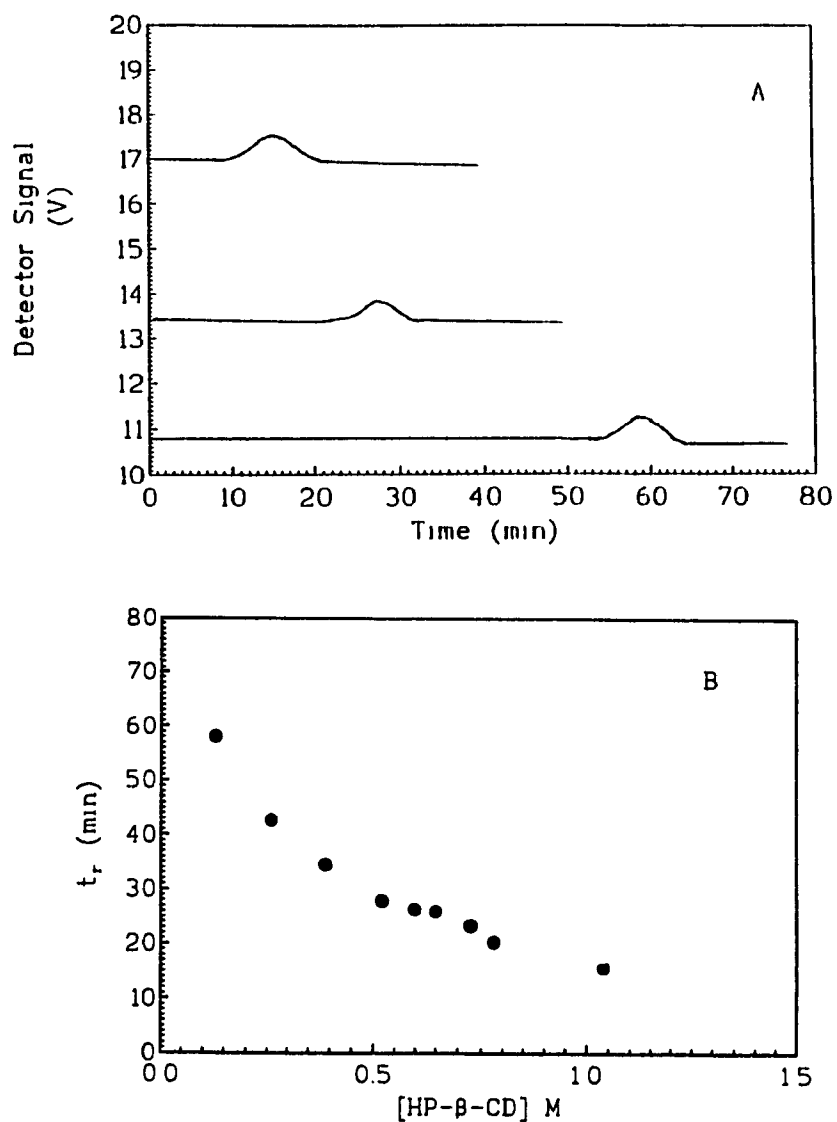
$\beta$ -CD was used to optimize the mobile-phase ANS concentration, since it binds less strongly than HP- $\beta$ -CD with ANS. Mobile phases containing  $10^{-8}$  to  $10^{-3}$  M ANS were tested, and  $\beta$ -CD solutions made with the mobile phase over the  $10^{-4}$  to  $10^{-2}$  M range were injected. Values of background ANS fluorescence and total fluorescence at the CD peak were measured, and these are given in Appendix 8. A plot of total peak fluorescence divided by background fluorescence (the signal-to-background ratio) vs  $\log[\text{ANS}]$  is shown in Figure 3.1. These results show that, at a mobile phase ANS concentration of  $10^{-4}$  M,  $\beta$ -CD is readily detected over the entire  $10^{-4}$  to  $10^{-2}$  M concentration range. At the lowest injected  $\beta$ -CD concentration,  $1.00 \times 10^{-4}$  M, a 50% increase in fluorescence is observed as  $\beta$ -CD elutes.

Thus, for an injected CD concentration of 5.0 mM under chromatographic conditions, even if a 50-fold dilution of injected CD occurs during elution from the column, retention times will be readily measurable with  $10^{-4}$  M ANS present in the mobile phase. At this concentration, 0.7% of the  $\beta$ -CD in a 5 mM solution (0.033 mM) exists as the ANS complex ( $K_a = 95 \text{ M}^{-1}$ , Chapter 2), and this does not significantly decrease the free  $\beta$ -CD concentration. Any contribution of ANS to decreased CD retention times will appear in the  $k'_0$  term of equation 4, and will cancel during the calculation of guest-CD association constants.

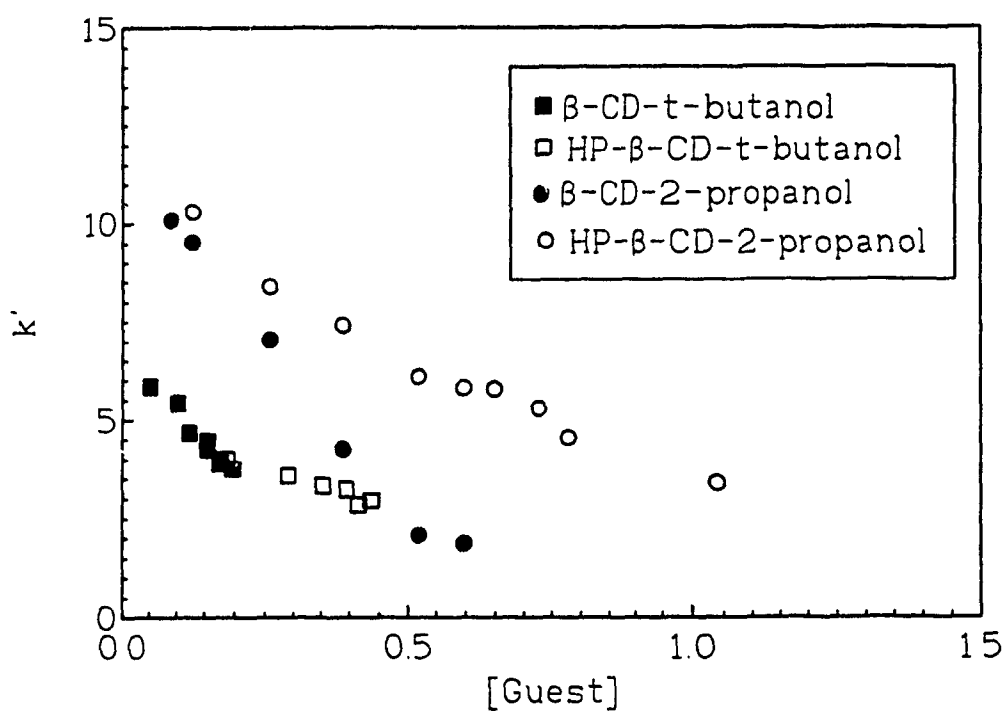
#### *Determination of association constants of CD-alcohol complexes*

Figure 3.2 shows typical chromatographic data, for the reaction of HP- $\beta$ -CD on a  $C_{18}$  stationary phase, as a function of 2-propanol concentration in the mobile phase.

In Figure 3.2 (A), the chromatograms show that the background fluorescence of



**Figure 3.2** (A) Chromatograms of 100  $\mu$ l injection of 5.00 mM HP- $\beta$ -CD-at different concentrations of 2-propanol. The concentrations of 2-propanol (M) are 0.13, 0.52 and 1.04 from bottom to top. (B) Plot of average retention time vs. [2-propanol] for injected HP- $\beta$ -CD.



**Figure 3.3** Capacity factor  $k'$  vs guest concentration, on a  $C_{18}$  column.

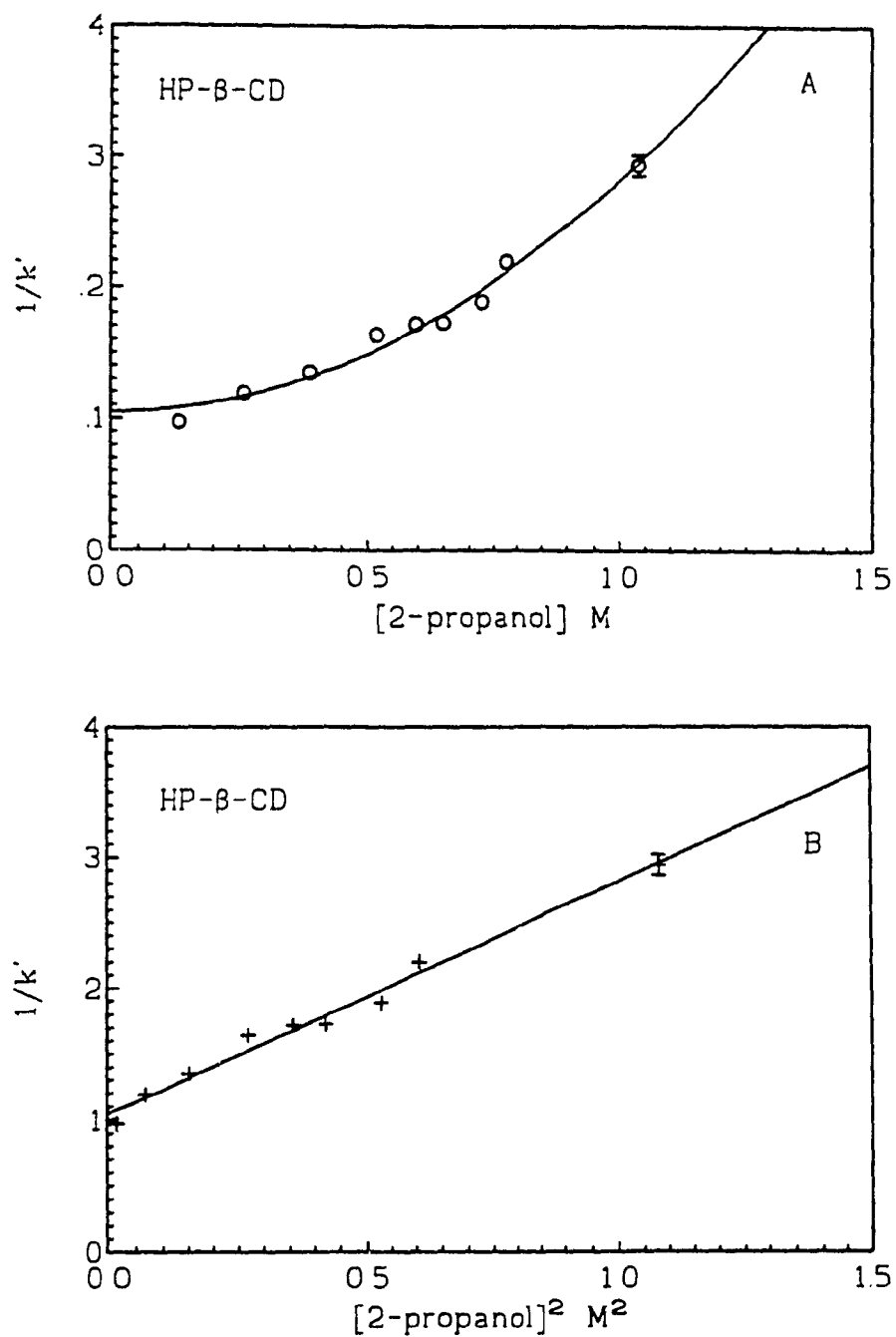


**Figure 3.4** Plots according to equation 4, of reciprocal capacity factor vs mobile phase guest (2-propanol) concentration, for HP- $\beta$ -CD retention assuming (a)  $n = 1$  and (b)  $n = 2$ .

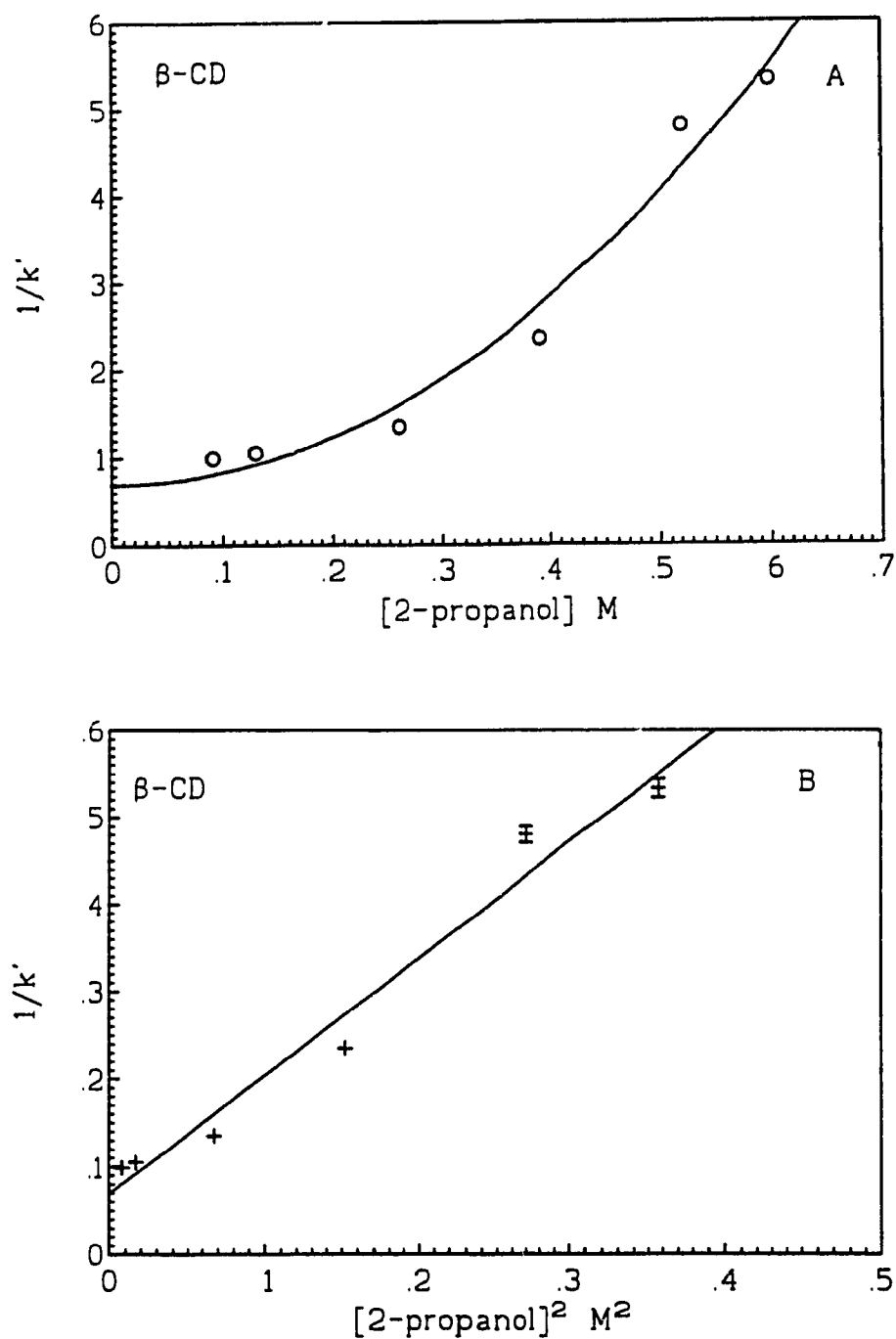


**Figure 3.5** Plots according to equation 4, of reciprocal capacity factor vs mobile phase guest (2-propanol) concentration, for  $\beta$ -CD retention assuming (a)  $n = 1$  and (b)  $n = 2$ .

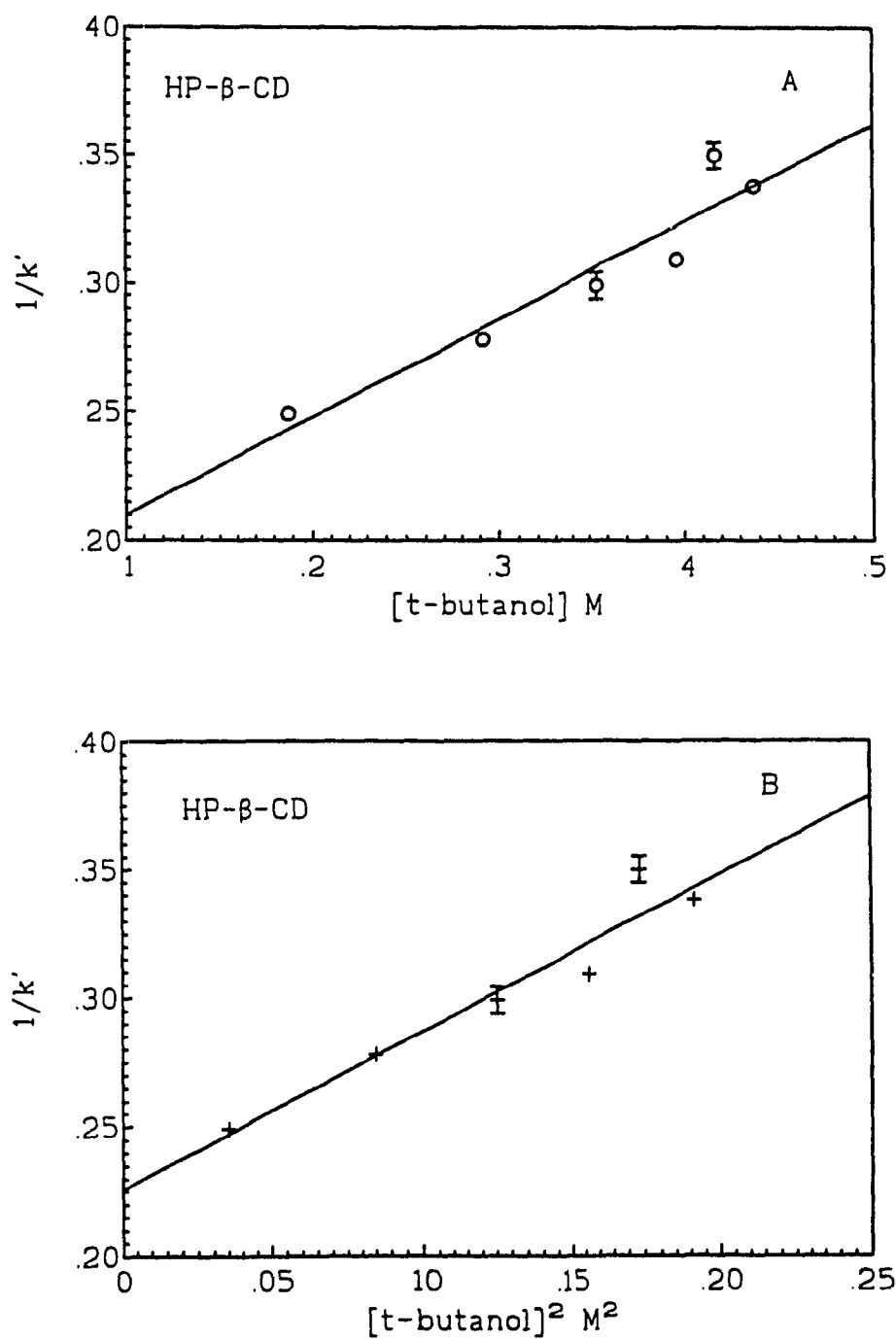


**Figure 3.6** Plots according to equation 4, of reciprocal capacity factor vs mobile phase guest (t-butanol) concentration, for HP- $\beta$ -CD retention assuming (a)  $n = 1$  and (b)  $n = 2$ .

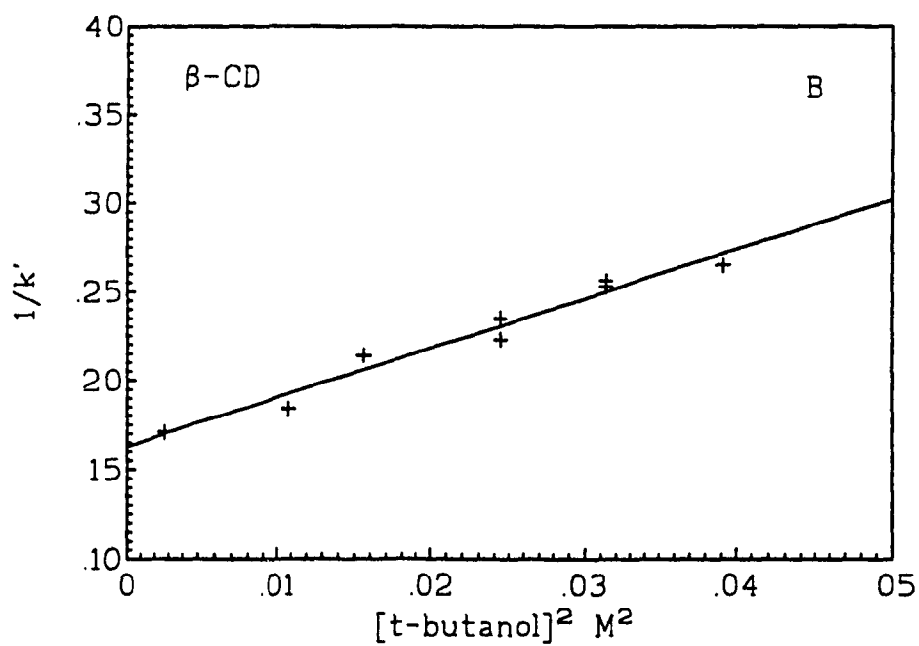
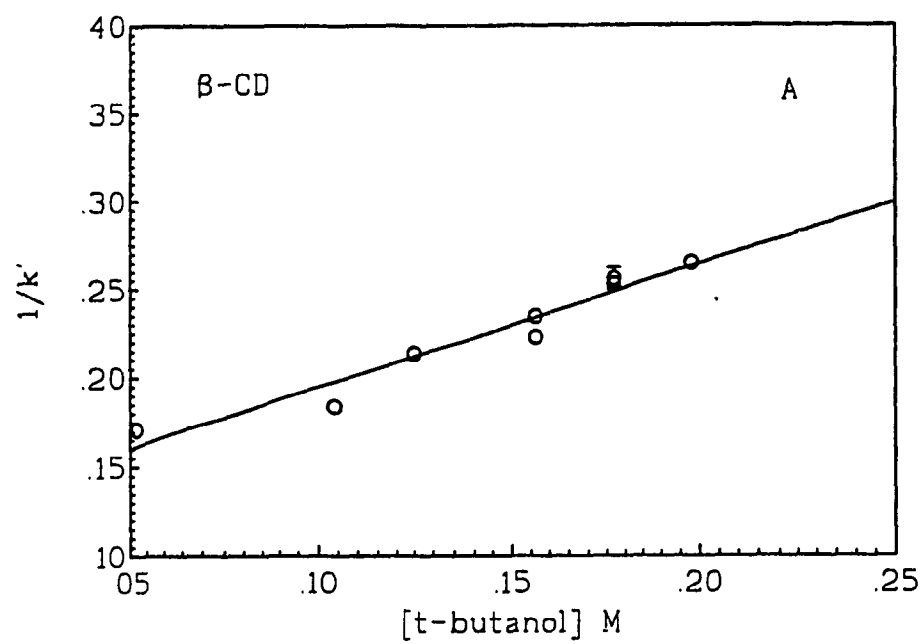


**Figure 3.7** Plots according to equation 4, of reciprocal capacity factor vs mobile phase guest (t-butanol) concentration, for  $\beta\text{-CD}$  retention assuming (a)  $n = 1$  and (b)  $n = 2$



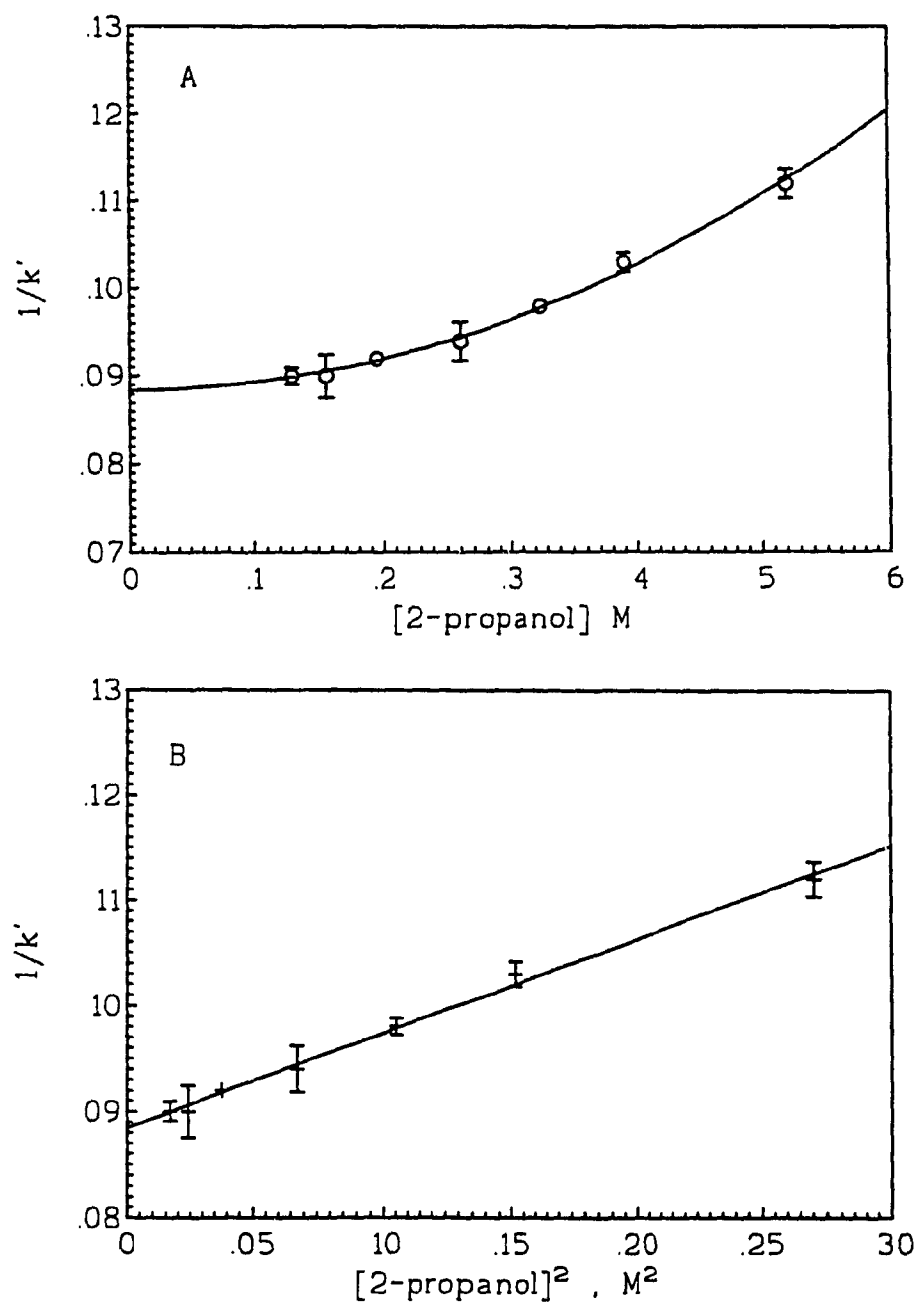


**Figure 3.8** Plots according to equation 4, of reciprocal capacity factor vs mobile phase guest (2-propanol) concentration, for HP- $\beta$ -CD retention on reversed-phase phenyl column assuming (a)  $n = 1$  and (b)  $n = 2$ .

ANS increases with the concentration of 2-propanol in the mobile phase. This also occurred when t-butanol was used as the mobile phase modifier, and results from the increasing hydrophobicity of the environment of free ANS. Over the 0.130 - 1.04 M range of 2-propanol, the retention time of HP- $\beta$ -CD decreases dramatically, from 58 to 16 minutes, while a non-retained species (water) exhibits an elution time that decreases slightly, from 5.1 to 3.6 minutes. At each 2-propanol concentration three replicate measurements were made, and capacity factors were calculated from the average  $t_r$  and  $t_0$  values. For HP- $\beta$ -CD, the  $k'$  values decreased from 10.3 to 3.39 as [2-propanol] increased from 0.130 to 1.04 M.

The complete data set for this system, as well as the  $\beta$ -CD-2-propanol, HP- $\beta$ -CD-t-butanol and  $\beta$ -CD-t-butanol experiments are given in Appendix 9. All of these data show a similar trend, with  $t_r$  (and  $k'$ ) values decreasing as the concentration of 2-propanol or t-butanol is increased. Figure 3.3 shows plots of  $k'$  vs [guest], for all four systems. These data support the model of competition between stationary phase  $C_{18}$  groups and mobile phase guest for the CD cavity, presented in Scheme 2 and quantified with equation 4.

Plots of  $1/k'$  against [guest]<sup>n</sup> according to equation 4, using n values of 1 and 2, are shown for each of the four systems, HP- $\beta$ -CD-2-propanol,  $\beta$ -CD-2-propanol, HP- $\beta$ -CD-t-butanol,  $\beta$ -CD-t-butanol, in Figures 3.4 - 3.7. Interestingly, linear plots are obtained for 2:1 guest:CD stoichiometry if 2-propanol is the guest, while linearity is seen for both 1:1 and 2:1 plots if t-butanol is the guest.

Many literature reports<sup>11,12,13</sup> have shown that long-chain alkyl groups are easily

included in the CD cavity because of their hydrophobic properties. Although the exterior of the CD is hydrophilic, the hydrophobic interaction of the CD cavity with the column allows CD retention on the column. CDs are also capable of including aromatic moieties, such as phenyl group of benzoic acid<sup>14</sup>. To support the proposed retention mechanism, one experiment was performed using a "phenyl" reversed-phase column. With this stationary phase, the  $C_{18}$  groups are replaced by pendant hydrophobic phenyl groups that should also be capable of retaining CDs by an inclusion mechanism. HP- $\beta$ -CD interacts as strongly with the phenyl stationary phase as it does with the  $C_{18}$  phase. For example, using a mobile phase containing 0.13 M 2-propanol, the average capacity factor was 11.1 on the phenyl column, while a value of 10.3 was obtained using the  $C_{18}$  column. Values of  $t_r$  and  $t_0$  differ between columns due to the different column dimensions.

Data for the retention of HP- $\beta$ -CD on a phenyl column at various mobile-phase 2-propanol concentrations are given at the end of Appendix 9, and Figure 3.8 shows plots of  $1/k'$  against  $[2\text{-propanol}]^n$  according to equation 4, for  $n = 1$  and  $n = 2$ . Again, the  $n = 2$  plot shows reasonable linearity, supporting the results obtained with the  $C_{18}$  stationary phase.

Equation 4 predicts that, for a correct choice of  $n$ , association constants are calculated as the slope/intercept ratio from the linear plot of  $1/k'$  against  $[\text{guest}]^n$ . Table 3.1 gives the calculated formation constants for the 2:1 2-propanol complexes and the 1:1 *t*-butanol complexes with HP- $\beta$ -CD and  $\beta$ -CD.

It can be seen in Table 3.1 that association constants determined by RPLC show that binding of 2-propanol with  $\beta$ -CD is slightly stronger than binding with HP- $\beta$ -CD.

This observation is consistent with the  $K_a$  values determined by the spectroscopic displacement method (Table 2.3, Chapter 2). Although only the t-butanol values can be directly compared, due to the assumed 1:1 binding stoichiometry, good agreement exists between the HP- $\beta$ -CD value of  $2.2 \pm 0.4 \text{ M}^{-1}$  (RPLC) and the value of  $2.0 \pm 0.1 \text{ M}^{-1}$  found by fluorescent probe displacement.

**Table 3.1**  $K_a$  values from reversed phase HPLC

Guest	$\beta$ -CD		HP- $\beta$ -CD	
	$K_a$	n	$K_a$	n
2-Propanol ( $C_{18}$ )	$19.4 \pm 6.4 \text{ M}^{-2}$	2	$1.7 \pm 0.1 \text{ M}^{-2}$	2
2-propanol (Phenyl)			$1.01 \pm 0.03 \text{ M}^{-2}$	2
t-Butanol ( $C_{18}$ )	$5.6 \pm 0.7 \text{ M}^{-1}$	1	$2.2 \pm 0.4 \text{ M}^{-1}$	1

For both  $\beta$ -CD and HP- $\beta$ -CD, the RPLC method shows that 2:1 2-propanol:CD binding stoichiometry exist. This information was not available from the spectroscopic displacement method, which assumes 1:1 binding and which used lower concentration of alcohol. Although it is more laborious, the RPLC method can thus provide more information about CD-guest association reactions than accepted spectroscopic methods.

### 3.4 References

- (1) Szejtli, J. *Cyclodextrin Technology*, Kluwer Academic Publishers, Dordrecht. 1988. p. 103.
- (2) Tee, O.S.; Du, X-X. *J. Am. Chem. Soc.* **1992**, 114, 620-627.
- (3) Kondo, H.; Nakatani, H.; Hiromi, K. *J. Biochem.*, **1976**, 79, 393-405.
- (4) Uekama, K.; Hirayama, F.; Nasu, S.; Matsuo, N.; Irie, T. *Chem. Pharm. Bull.*, **1978**, 26, 3477
- (5) Mohseni, R.M.; Hurtubise, R.J. *J. Chromatogr.* **1990**, 499, 395-410.
- (6) Anigbogu, V.C.; Muñoz de la Peña, A.; Ndou, T.T.; Warner, I.M. *Anal. Chem.*, **1992**, 64, 484-489.
- (7) Koizumi, K.; Kubota, Y.; Okada, Y.; Utamura, T. *J. Chromatogr.*, **1988**, 437, 47-57.
- (8) Ueno, A.; Breslow, R. *Tetrahedron Letters*, **1982**, 23, 3451-3454.
- (9) Tabushi, I.; Shimizu, N.; Sugimoto, T.; Shiozuka, M.; Yamamura, K. *J. Am. Chem. Soc.*, **1977**, 99, 7100-7102.
- (10) Breslow, R.; Greenspoon, N.; Guo, T.; Zarzycki, R. *J. Am. Chem. Soc.*, **1989**, 111, 8296-8297.
- (11) Matsui, Y.; Mochida, K. *Bull. Chem. Soc. Jpn.*, **1979**, 52, 2808- 2814.
- (12) Tee, O.S.; Mazza, C.; Lozano-Hemmer, R.; Giorgi, J.B. *J. Org. Chem.*, **1994**, 59, 7602-7608.
- (13) Tee, O.S.; Gadosy, T.A. *J. Chem. Soc. Perkin Trans. 2*, **1994**, 2307-2311.
- (14) Bender, M.I.; Komiyama, M. *Cyclodextrin Chemistry* ; Springer-Verlag: New

York, 1978. pp 10-12.

## 5. Summary and Suggestions for Future Work

All values of association constants determined in this work, and literature values for comparison, are shown in Table 4.1. From these results we can see the values for CD-ANS complexes obtained by direct fluorescence measurements are consistent with the literature values. The association constants for  $\beta$ -CD-t-butanol or  $\beta$ -CD-2-propanol complexes obtained by the fluorescence displacement method are consistent with the literature values where a similar spectroscopic displacement method was used. However, association constant for HP- $\beta$ -CD-t-butanol and HP- $\beta$ -CD-2-propanol complexes show a large discrepancy with literature values, where an inhibition kinetics method was used under very basic conditions (pH 11.6). When we compare values obtained by RP-HPLC with the spectroscopic displacement method, we notice that the  $K_a$  value for the HP- $\beta$ -CD-t-butanol complex are similar by these two different methods. Both show a discrepancy from the literature values. Although there are discrepancies between these results and literature values this new HPLC method provides more information about the host-guest binding. For both CD-2-propanol complexes, 1:2 stoichiometry was obtained. This stoichiometry is reasonable because 2-propanol is smaller than the bulky t-butanol guest, and can interact with CD both by entering the cavity and interacting with the periphery of the cavity. It can also be concluded, from both RP-HPLC and fluorescence displacement methods, that  $\beta$ -CD binding is stronger than HP- $\beta$ -CD binding with 2-

**Table 4.1** Summary of  $K_a$  values

Host	Guest	Method <sup>a</sup>	$K_a$ ( $M^{-1}$ )	Lit Values
$\alpha$ -CD	ANS	F	$9 \pm 1$	$5^7, 2^7$
$\beta$ -CD	ANS	F	$95 \pm 9$	$110^2, 95^3, 77^4, 65^1, 64^5$
	2-propanol	FD	$6.1 \pm 1.0$	$3.8^6$
		RPLC	$19.4 \pm 6.4$ (n = 2)	
	t-butanol	FD	$45.6 \pm 0.8$	$47.9^6$
		RPLC	$5.6 \pm 0.7$	
HP- $\beta$ -CD	ANS	F	$420 \pm 5$	$585^7$
	2-propanol	FD	$0.8 \pm 0.4$	$3.6^8$
		RPLC	$1.7 \pm 0.1$ (n = 2)	
	t-butanol	FD	$2.0 \pm 0.1$	$25^8$
		RPLC	$2.2 \pm 0.4$	

<sup>a</sup>F, FD and RPLC indicate Fluorescence, Fluorescence displacement and Reversed-phase HPLC method respectively.



propanol.

In this work the suggested mechanism for CD binding with alcohols is not confirmed by either the RP-HPLC or the displacement method. Direct evidence could be obtained by nuclear magnetic resonance (NMR), and a ternary ANS-CD-alcohol complex could also be detected by changes in the chemical shifts of CDs or guests.

Normally, the derivatives of CDs are expected to contain several components with various degrees of substitution, so actually they are a mixture. In order to study the binding behaviour of these components with selected guest species, the components must be separated first. Using the new HPLC method, the components of these mixtures could be separated, and characterized with respect to guest binding, and identified with only one experimental procedure, if a mass spectrometric detector were used. The advantage of this new HPLC method is that a very small amount of CD is used, and at the same time as the separation occurs, the association constants and stoichiometry of inclusion complexes can be determined.

## References

- (1) Schneider, H-J.; Blatter, T.; Simova, S. *J. Am. Chem. Soc.*, **1991**, 113, 1996-2000.
- (2) Catena, G. C.; Bright, F.V.; *Anal. Chem.*, **1989**, 61, 905-909.
- (3) Aoyama, Y.; Nagai, Yoshiro.; Otsuki, J-I.; Kobayashi, K.; Toi, H. *Angew. Chem. Int. Ed. Engl.*, **1992**, 31, 745-747.
- (4) Tabushi, N.; Shimizu, T.; Sugimoto, M.; Shiozuka, K.Y.; *J. Am. Chem. Soc.*, **1977**, 99, 7100-7102.
- (5) Franke, J.; Merz, F.; Lorensky, H. W.; Muller, W. M.; Wermer, W.; Vögtle, F.; *J. Inclusion Phenom.*, **1985**, 3, 471 - 478.
- (6) Matsui, Y; Mochida, K. *Bull. Chem. Soc. Jpn.*, **1979**, 52, 2808- 2814.
- (7) Tee, O.S.; Gadosy, T.A.; Giorgi, J.B. Submitted to *Can. J. Chem.*, (1995)
- (8) Tee, O.S.; Gadosy, T.A.; Giorgi, J.B. *J. Chem. Soc. Perkin Trans. 2*, **1993**, 1705-1706.

## Appendix 1

### Linear Regression (Scatchard) Method

For a simple equilibrium



$$K_a = [\text{ANS-CD}]/[\text{ANS}][\text{CD}] \quad (1)$$

The total concentration of ANS is  $[\text{ANS}]_0$ , and the total concentration of CD is  $[\text{CD}]_0$ ,

so we obtain:

$$[\text{ANS}]_0 = [\text{ANS}] + [\text{ANS-CD}] \quad (2)$$

$$\text{and } [\text{CD}]_0 = [\text{CD}] + [\text{ANS-CD}]. \quad (3)$$

As we know the fluorescence intensity is directly proportional to the sample concentration, so the total fluorescence intensity is the sum of fluorescence intensities of free ANS and the ANS-CD complex:

$$\begin{aligned} I &= I_{\text{ANS}} + I_{\text{ANS-CD}} \\ &= k[\text{ANS}] + k'[\text{ANS-CD}], \end{aligned} \quad (4)$$

where  $k'$  and  $k$  are constants under a given set of experimental conditions.

Substituting equation (2) into equation (4) yields

$$\begin{aligned}
I &= k ([\text{ANS}]_0 - [\text{ANS-CD}]) + k'[\text{ANS-CD}] \\
&= k'[\text{ANS-CD}] - k[\text{ANS-CD}] + k[\text{ANS}]_0 \\
&= [k' - k][\text{ANS-CD}] + I_0.
\end{aligned} \tag{5}$$

Rearranging equation (5) yields

$$(I - I_0)/(k' - k) = [\text{ANS-CD}], \tag{6}$$

$$\Delta I/\Delta k = [\text{ANS-CD}], \tag{7}$$

where  $\Delta I = I - I_0$  and  $\Delta k = k' - k$ . Rearranging equation (1) gives

$$[\text{ANS-CD}] = K_a[\text{ANS}][\text{CD}]. \tag{8}$$

Rearranging equation (2) gives

$$[\text{ANS}] = [\text{ANS}]_0 - [\text{ANS-CD}]. \tag{9}$$

Substituting equation (9) and (8) into equation (7) yields

$$\Delta I/\Delta k = K_a ([\text{ANS}]_0 - [\text{ANS-CD}])[\text{CD}]. \tag{10}$$

Rearranging equation (10) yields

$$\Delta I/(\Delta k[CD]) = K_a([ANS]_0 - [ANS-CD]). \quad (11)$$

Substituting equation (7) into equation (11) and then rearranging yields

$$\Delta I/[CD] = K_a \Delta k [ANS]_0 - K_a \Delta I. \quad (12)$$

Equation (12) is simplified by considering that  $[CD]_0 \gg [ANS]_0$  and  $[CD]_0 \gg [ANS-CD]$ , so that  $[CD]_0$  can be considered equal to  $[CD]$ , and the final expression (13) is obtained:

$$\begin{aligned} \Delta I/[CD]_0 &= K_a \Delta k [ANS]_0 - K_a \Delta I \\ &= K_a C [ANS]_0 - K_a \Delta I \end{aligned} \quad (13)$$

where  $C = \Delta k$ . From equation (13), a plot of  $\Delta I/[CD]_0$  versus  $\Delta I$  should give a straight line with a slope of  $-K_a$ . The computer program InPlot 4 (Graph Pad) gives the  $K_a$  value with uncertainty.

## **Appendix 2**

### **Non-linear Regression Method**

**For a simple equilibrium**



$$K_d = [\text{CD}][\text{ANS}]/[\text{ANS-CD}]. \quad (1)$$

**In the absence of CD, the fluorescence intensity of ANS at a fixed wavelength is**

$$I_0 = k[\text{ANS}]_0. \quad (2)$$

**In the presence of CD, the total fluorescence intensity is the sum of the fluorescence intensities of free ANS and the complex ANS-CD:**

$$\begin{aligned} I &= k[\text{ANS}] + k'[\text{ANS-CD}] \\ &= k[\text{ANS}] + k' ([\text{ANS}]_0 - [\text{ANS}]). \end{aligned} \quad (3)$$

**When all ANS is bound to CD, the total concentration of complex is equal to the total concentration of ANS, so the fluorescence intensity is:**

$$I_b = k'[\text{ANS}]_0. \quad (4)$$

From equation (2) & equation (4), equation (5) is obtained:

$$I_0 - I_b = (k - k')[ANS]_0. \quad (5)$$

From equation (3) & equation (4), equation (6) is obtained:

$$I - I_b = (k - k')[ANS]. \quad (6)$$

Combining (5) with equation (6), equation (7) is obtained:

$$I_0 - I = (k - k')([ANS]_0 - [ANS]). \quad (7)$$

Since  $[ANS]_0 = [ANS] + [ANS-CD]$ , equation (7) becomes

$$I_0 - I = (k - k') [ANS-CD]. \quad (8)$$

Combining equation (6), with equation (8), equation (9) is obtained:

$$[ANS]/[ANS-CD] = (I - I_b)/(I_0 - I). \quad (9)$$

Rearranging equation (1) yields

$$[\text{ANS}]/[\text{ANS-CD}] = K_d/[\text{CD}], \quad (10)$$

and substituting equation (9) gives equation (11):

$$I = (I_0K_d + I_b[\text{CD}])/(K_d + [\text{CD}]) \quad (11)$$

Equation (11) is simplified by considering that  $[\text{CD}]_0 \gg [\text{ANS}]_0$  and  $[\text{CD}]_0 \gg [\text{ANS-CD}]$ , so that  $[\text{CD}]_0$  can be considered equal to  $[\text{CD}]$ , and the final expression (12) is obtained:

$$I = (I_0K_d + I_b[\text{CD}]_0)/(K_d + [\text{CD}]_0). \quad (12)$$

In this method  $K_d$ ,  $I_0$  and  $I_b$  are considered to be parameters. The non-linear regression program begins with proposed values for the three parameters in equation (12), and the values of these parameters are adjusted iteratively until the selected equation fits the data best, so that the  $K_d$  value can be obtained. Because  $I$  is the measured fluorescence intensity at a fixed wavelength, and  $[\text{CD}]_0$  is known, the non-linear regression method based on equation (12) can be used to get  $K_d$ . The computer program InPlot 4 (Graph Pad) gives the  $K_d$  value with uncertainty.



### Appendix 3

#### Spectroscopic Displacement Method

Consider the following two equilibria:



$$K_d = [\text{ANS}] [\text{CD}] / [\text{ANS-CD}] \quad (2)$$



$$K_d' = [\text{A}] [\text{CD}] / [\text{A-CD}], \quad (4)$$

where A is a spectroscopically invisible guest, such as 2-propanol or t-butanol. The total concentration of ANS is given by:

$$[\text{ANS}]_0 = [\text{ANS}] + [\text{ANS-CD}] \quad (5)$$

The measured fluorescence intensity will always be given by:

$$I = k'[\text{ANS}] + k [\text{ANS-CD}] \quad (6)$$

$$= k'[\text{ANS}]_0 + (k - k')[\text{ANS-CD}] \quad (7)$$

When no alcohol is present,  $[\text{CD}] = [\text{CD}]_0 - [\text{ANS-CD}]$ , and substituting this and  $[\text{ANS}]$

$= [\text{ANS}]_0 - [\text{ANS-CD}]$  into eq. 2,

$$K_d = ([CD]_0 - [ANS-CD])([ANS]_0 - [ANS-CD])/[ANS-CD]$$

Since  $[CD]_0 \gg [ANS]_0 > [ANS-CD]$ ,

$$K_d = [CD]_0([ANS]_0 - [ANS-CD])/[ANS-CD] \quad (8)$$

Eq. 8 rearranges to

$$[ANS-CD] = [CD]_0[ANS]_0/(K_d + [CD]_0) \quad (9)$$

Substituting into eq. 7 yields

$$I = k'[ANS]_0 + (k - k') [CD]_0[ANS]_0/(K_d + [CD]_0) \quad (10)$$

When alcohol is present,

$$K_d' = [CD][A]/[A-CD] = [CD]([A]_0 - [A-CD])/[A-CD] \quad (11)$$

Since  $[A]_0 \gg [CD]_0 > [A-CD]$ ,

$$K_d' = [CD][A]_0/[A-CD] \quad (12)$$

Since  $[CD]_0 = [CD] + [ANS-CD] + [A-CD]$ ,

$$[CD]_0 = [CD] + [ANS-CD] + [CD][A]_0/K_d' \quad (13)$$

Solving for  $[CD]$  yields

$$[CD] = ([CD]_0 - [ANS-CD])/(1 + [A]_0/K_d') \quad (14)$$

Since  $[CD]_0 \gg [ANS]_0 > [ANS-CD]$ ,

$$[CD] = [CD]_0/(1 + [A]_0/K_d') \quad (15)$$

From eq. 2,

$$K_d = [ANS] [CD] / [ANS-CD]$$

so

$$[CD] = K_d [ANS-CD]/[ANS] = K_d [ANS-CD]/([ANS]_0 - [ANS-CD]) \quad (16)$$

Setting eq. 15 equal to eq. 16,

$$[CD]_0/(1 + [A]_0/K_d') = K_d [ANS-CD]/([ANS]_0 - [ANS-CD]) \quad (17)$$

Rearranging eq. 17 to solve for [ANS-CD],

$$[\text{ANS-CD}] = K_d'[\text{CD}]_0[\text{ANS}]_0 / \{K_d[A]_0 + K_d'(K_d + [\text{CD}]_0)\} \quad (18)$$

Substituting into eq. 7 yields

$$I = k'[\text{ANS}]_0 + (k - k')K_d'[\text{CD}]_0[\text{ANS}]_0 / [K_d[A]_0 + K_d'(K_d + [\text{CD}]_0)] \quad (19)$$

The measured fluorescence intensity difference  $\Delta I$  is then eq. 19 minus eq. 10

$$\begin{aligned} \Delta I = & (k - k') \{ K_d'[\text{CD}]_0[\text{ANS}]_0 / [K_d[A]_0 + K_d'(K_d + [\text{CD}]_0)] \\ & - [[\text{CD}]_0[\text{ANS}]_0 / (K_d + [\text{CD}]_0)] \}. \end{aligned} \quad (20)$$

Eq. 20 rearranges to eq. 21,

$$\Delta I = (k - k') [\text{ANS}]_0 [\text{CD}]_0 [A]_0 / [A]_0 K_d (K_d + [\text{CD}]_0) + K_d' (K_d + [\text{CD}]_0)^2, \quad (21)$$

and the reciprocal of eq. 21 yields the final expression:

$$\begin{aligned} 1/\Delta I = & [K_d' (K_d + [\text{CD}]_0)^2 / (k - k') [\text{ANS}]_0 [\text{CD}]_0] (1/[A]_0) \\ & + K_d (K_d + [\text{CD}]_0) / (k - k') [\text{ANS}]_0 [\text{CD}]_0 \end{aligned} \quad (22)$$

Thus, a plot  $1/\Delta I$  against  $1/[A]_0$  yields a slope/y-intercept ratio equal to  $K_d'(K_d + [CD]_0)/K_d$ , where  $K_d$  and  $[CD]_0$  are known. So the final equation is obtained:

$$K_d' = [K_d/(K_d + [CD]_0)] * \text{slope/intercept.} \quad (23)$$

Because  $K_d$  and  $[CD]_0$  are known constants,  $K_d'$  can be calculated using equation (23). The computer program InPlot 4 (Graph Pad) gives the standard error for both slope and intercept and then the uncertainty of  $K_d$  can be calculated.

#### Appendix 4

##### Fluorescence intensity of ANS with $\alpha$ -CD <sup>a</sup>

[ $\alpha$ -CD] (M)	I <sub>1</sub>	I <sub>2</sub>	I <sub>3</sub>	I <sub>avg</sub> <sup>b</sup>	$\Delta I$ <sup>c</sup>	$\Delta I/[\alpha\text{-CD}]$ $\times 10^{-3}$
0.00	11.26	11.07	11.07	11.13		
$4.00 \times 10^{-4}$	12.67	12.60	12.60	12.62		
$8.00 \times 10^{-4}$	13.69	13.69	13.69	13.69		
$1.00 \times 10^{-3}$	14.20	14.20	14.14	14.18		
$4.80 \times 10^{-3}$	23.10	23.87	22.84	23.27	12.14	2.529
$7.20 \times 10^{-3}$	28.86	29.12	28.73	28.90	17.77	2.468
$9.60 \times 10^{-3}$	33.98	34.24	34.49	34.24	23.11	2.407
$1.92 \times 10^{-2}$	54.20	53.69	54.20	54.03	42.90	2.234
$2.88 \times 10^{-2}$	67.00	70.84	70.08	69.31	58.18	2.020
$3.84 \times 10^{-2}$	85.18	84.67	85.18	85.01	73.88	1.924

<sup>a</sup> Measured at excitation wavelength of 368.0 nm and emission wavelength of 494.4 nm.

<sup>b</sup> The average of three measured fluorescence intensities.

<sup>c</sup> Calculated by I<sub>avg</sub> in presence of  $\alpha$ -CD minus I<sub>avg</sub> in absence of  $\alpha$ -CD.

Fluorescence intensity of ANS with  $\beta$ -CD<sup>a</sup>

[ $\beta$ -CD] (M)	I <sub>1</sub>	I <sub>2</sub>	I <sub>3</sub>	I <sub>avg</sub> <sup>b</sup>	$\Delta I^c$	$\Delta I/[\beta\text{-CD}]$ x 10 <sup>-4</sup>
0.00	9.15	9.15	9.4	9.23		
1.00 x 10 <sup>-4</sup>	10.75	10.68	10.62	10.68		
2.00 x 10 <sup>-4</sup>	12.35	12.35	12.67	12.46		
4.00 x 10 <sup>-4</sup>	16.12	16.12	16.19	16.14	6.91	1.73
6.00 x 10 <sup>-4</sup>	18.88	19.00	19.64	19.17	9.94	1.66
8.00 x 10 <sup>-4</sup>	22.20	22.08	23.10	22.46	13.23	1.65
1.00 x 10 <sup>-3</sup>	25.40	24.38	26.17	25.32	16.09	1.61
4.00 x 10 <sup>-3</sup>	68.54	67.52	69.82	68.63	59.40	1.48
6.00 x 10 <sup>-3</sup>	83.13	85.18	84.67	84.33	75.10	1.25
8.00 x 10 <sup>-3</sup>	97.47	97.47	103.61	99.52	90.29	1.13

<sup>a</sup> Measured at excitation wavelength of 368.0 nm and emission wavelength of 490.0 nm.

<sup>b</sup> The average of three measured fluorescence intensities.

<sup>c</sup> Calculated by I<sub>avg</sub> in presence of  $\beta$ -CD minus in absence of  $\beta$ -CD.

Fluorescence intensity of ANS with HP-  $\beta$ -CD<sup>a</sup>

[HP- $\beta$ -CD] (M)	I <sub>1</sub>	I <sub>2</sub>	I <sub>3</sub>	I <sub>avg</sub> <sup>b</sup>	$\Delta I^c$	$\Delta I/[HP-\beta-CD]$ $\times 10^{-4}$
0.00	0.57	0.57	0.57	0.57		
$1.00 \times 10^{-4}$	13.31	13.05	13.31	13.22	12.65	12.65
$3.00 \times 10^{-4}$	37.63	39.93	39.42	38.99	38.42	12.81
$6.00 \times 10^{-4}$	70.65	70.65	70.65	70.65	70.08	11.68
$8.00 \times 10^{-4}$	87.04	87.04	88.06	87.38	86.81	10.85
$1.20 \times 10^{-3}$	116.73	114.68	115.71	115.71	115.14	9.59
$2.40 \times 10^{-3}$	174.08	175.10	176.12	175.10	174.53	7.27
$4.00 \times 10^{-3}$	219.13	219.13	220.16	219.47	218.90	5.47
$6.00 \times 10^{-3}$	252.92	247.80	249.85	250.19	249.62	4.16
$8.00 \times 10^{-3}$	267.26	267.26	267.26	267.26	266.69	3.33

<sup>a</sup> Measured at excitation wavelength of 368.0 nm and emission wavelength of 468.0 nm.

<sup>b</sup> The average of three measured fluorescence intensities.

<sup>c</sup> Calculated by I<sub>avg</sub> in presence of HP- $\beta$ -CD minus I<sub>avg</sub> in absence of HP- $\beta$ -CD.



## **Appendix 5**

Fluorescence Intensity<sup>a</sup> of  $1.00 \times 10^{-4}$  M ANS at Different pH

pH	Fluorescence Intensity	pH	Fluorescence Intensity
3.857	83.96	6.122	78.33
4.060	83.45	6.304	79.36
4.280	83.45	6.516	79.87
4.471	83.96	6.748	79.87
4.686	82.94	6.914	78.84
4.852	82.94	7.016	79.36
5.044	81.40	7.222	79.87
5.254	83.45	7.397	78.84
5.460	83.45	7.734	78.84
5.664	81.92	7.890	79.87
5.859	83.45		

<sup>a</sup> Fluorescence Intensity was measured at excitation wavelength of 368.0 nm and emission wavelength of 512.0 nm. Excitation and emission band widths are 5.0 nm and 3.0 nm, respectively. Acetate buffer and phosphate buffer were used to prepare solutions of different pH.

Fluorescence Intensity<sup>a</sup> of  $1.00 \times 10^{-4}$  M ANS and  $5.0 \times 10^{-3}$  M  $\beta$ -CD at Different pH

pH	Fluorescence Intensity	pH	Fluorescence Intensity
3.904	173.05	6.082	186.36
4.123	166.91	6.281	185.34
4.341	174.08	6.499	186.36
4.735	177.15	6.734	183.29
4.902	178.17	6.901	185.34
5.107	185.34	7.003	184.32
5.308	185.34	7.207	181.24
5.508	186.36	7.395	183.29
5.666	185.34	7.727	181.24
5.819	186.36	7.858	183.29

<sup>a</sup> Fluorescence Intensity was measured at excitation wavelength of 368.0 nm and emission wavelength of 490.0 nm. Excitation and emission band widths are 5.0 nm and 3.0 nm, respectively. Acetate buffer and phosphate buffer were used to prepare solutions of different pH.

Fluorescence Intensity<sup>a</sup> of  $1.00 \times 10^{-4}$  M ANS and  $5.0 \times 10^{-3}$  M HP- $\beta$ -CD at Different pH

pH	Fluorescence Intensity	pH	Fluorescence Intensity
3.947	215.04	5.904	230.40
4.135	220.16	6.123	236.54
4.349	221.18	6.302	240.64
4.539	219.13	6.741	241.66
4.745	224.25	6.912	241.66
4.909	223.23	7.216	239.61
5.118	223.23	7.402	244.73
5.323	226.30	7.730	243.71
5.513	227.32	7.886	244.74
5.721	227.32		

<sup>a</sup> Fluorescence Intensity was measured at excitation wavelength of 368.0 nm and emission wavelength of 468.0 nm. Excitation and emission band widths are 1.5 nm and 3.0 nm, respectively. Acetate buffer and phosphate buffer were used to prepare solutions of different pH.

## Appendix 6

Fluorescence intensity of HP- $\beta$ -CD-ANS in presence of t-butanol<sup>a</sup>

[t-butanol] M	I1	I2	I3	$I_{avg}^b$
0.0	224.25	227.32	229.37	226.98
0.05	210.94	209.92	210.94	210.60
0.15	179.2	181.24	174.08	178.17
0.25	143.36	147.45	148.48	146.43
0.40	114.68	113.15	112.64	113.49
0.50	99.32	98.81	100.86	99.66
0.60	83.96	86.01	86.52	85.50
0.70	75.26	76.8	75.26	75.77
0.80	68.6	68.09	68.09	68.26

<sup>a</sup>Measured at  $[ANS]_0 = 1.0 \times 10^{-4}$  M and  $[HP-\beta-CD] = 8.0 \times 10^{-3}$  M with excitation wavelength of 368.0 nm and emission wavelength of 468.0 nm.

<sup>b</sup>The average of three measured fluorescence intensities.

Fluorescence intensity of  $\beta$ -CD-ANS in presence of t-butanol<sup>a</sup>

[t-butanol]	I1	I2	I3	I <sub>avg</sub> <sup>b</sup>
0.0	187.39	186.36	186.36	186.70
0.020	131.07	133.12	131.07	131.75
0.040	106.49	105.47	107.54	106.50
0.060	93.18	94.20	95.23	94.20
0.080	87.04	86.01	86.01	86.35
0.10	79.87	81.92	80.89	80.89
0.12	74.75	74.43	75.45	74.88
0.13	73.92	74.43	72.89	73.75
0.14	71.87	72.89	72.89	72.55

<sup>a</sup>Measured at  $[\text{ANS}]_0 = 1.0 \times 10^{-4} \text{ M}$  and  $[\beta\text{-CD}] = 4.2 \times 10^{-3} \text{ M}$  with excitation wavelength of 368.0 nm and emission wavelength of 490.0 nm.

<sup>b</sup>The average of three measured fluorescence intensities.

Fluorescence intensity of HP- $\beta$ -CD-ANS in presence of 2-propanol<sup>a</sup>

[2-propanol] M	I1	I2	I3	$I_{avg}^b$
0.00	264.19	264.19	265.21	264.53
0.125	247.80	247.80	247.80	247.80
0.146	244.73	245.76	244.73	245.07
0.166	243.71	241.66	242.68	242.68
0.187	240.64	240.64	240.64	240.64
0.312	225.28	225.28	223.23	224.60
0.624	186.36	184.32	186.36	185.68
0.832	165.88	162.81	162.81	163.83
1.04	148.48	147.45	147.45	147.79

<sup>a</sup>Measured at  $[ANS]_0 = 1.0 \times 10^{-4}$  M and  $[HP-\beta-CD] = 8.0 \times 10^{-3}$  M with excitation wavelength of 368.0 nm and emission wavelength of 468.0 nm.

<sup>b</sup>The average of three measured fluorescence intensities.

Fluorescence intensity of  $\beta$ -CD-ANS in presence of 2-propanol<sup>a</sup>

[2-Propanol] (M)	I1	I2	I3	$I_{\text{avg}}$ <sup>b</sup>
0.0	242.68	242.68	244.73	243.36
0.624	206.84	205.82	207.87	206.84
0.125	183.29	183.29	184.32	183.63
0.187	165.88	166.91	166.91	166.57
0.312	142.33	144.38	144.38	143.70
0.624	116.73	116.73	116.73	116.73
0.936	106.49	108.54	106.48	107.17
1.14	104.96	108.54	105.98	106.49

<sup>a</sup>Measured at  $[\text{ANS}]_0 = 1.0 \times 10^{-4} \text{ M}$  and  $[\beta\text{-CD}] = 4.2 \times 10^{-3} \text{ M}$  with excitation wavelength of 368.0 nm and emission wavelength of 490.0 nm.

<sup>b</sup>The average of three measured fluorescence intensities.

## Appendix 7

### HPLC Method for $K_a$ determination

The capacity factor of CD in reversed phase HPLC is defined as

$$k'_{\text{obs}} = (t_r - t_0)/t_0 = \phi[\text{CD}]_{\text{S,T}}/[\text{CD}]_{\text{M,T}}, \quad (1)$$

where  $t_r$  is the retention time of CD,  $t_0$  is the time required by an unretained species to travel from injector to detector,  $\phi$  is the volume ratio of stationary phase to mobile phase (a constant for a given column), and  $[\text{CD}]_{\text{S,T}}$  and  $[\text{CD}]_{\text{M,T}}$  are the total CD concentration in the stationary phase and the mobile phase, respectively.

From the inverse of equation (1), we obtain

$$1/k'_{\text{obs}} = [\text{CD}]_{\text{M,T}}/\phi[\text{CD}]_{\text{S,T}} \quad (2)$$

In the absence of mobile phase modifier, the capacity factor  $k'_0$  is given by equation (3).

$$k'_0 = \phi[\text{CD}]_{\text{S}}/[\text{CD}]_{\text{M}} \quad (3)$$

In the presence of a modifier, M, such as 2-propanol or t-butanol, the total CD concentration in the mobile phase is given by the following equation:

$$[\text{CD}]_{\text{M,T}} = [\text{CD}]_{\text{M}} + [\text{CD}-(\text{M})_n], \quad (4)$$



where  $[CD]_M$  is the free CD concentration in the mobile phase and  $[CD-(M)_n]$  is the concentration of CD-modifier complex in the mobile phase. The subscript n refers to the modifier:CD stoichiometry for the association reaction



Substituting (4) into (2) we obtain :

$$1/k'_{obs} = ([CD]_M + [CD-(M)_n]_M) / \phi [CD]_{S,T} \quad (6)$$

Assuming that only free CD can interact with the stationary phase,  $[CD]_{S,T}$  can be considered equal to  $[CD]_S$ , and equation (6) becomes

$$1/k'_{obs} = ([CD]_M + [CD-(M)_n]_M) / \phi [CD]_S \quad (7)$$

Substituting equation (3) into equation (6) yields

$$1/k'_{obs} = 1/k'_0 (1 + [CD-(M)_n]_M / [CD]_M) \quad (8)$$

Reaction (5) has, by definition, a association constant of:

$$K_n = [CD-(M)_n]_M / [CD]_M [M]^n \quad (9)$$

Substituting equation (9) into equation (8) yields the final equation

$$1/k'_{\text{obs}} = 1/k'_0(1 + K_a[M]_M^n) \quad (10)$$

Values of  $k'_{\text{obs}}$  are obtained by chromatography of injected CDs, using various mobile phase modifier concentrations  $[M]_M$ . For a correctly-chosen stoichiometry  $n$ , a plot of  $1/k'_{\text{obs}}$  against  $[M]_M^n$  should give a straight line with a slope/y-intercept ratio of  $K_d$ .

## Appendix 8

### Results from flow injection<sup>a</sup>

[ANS] (M)	1.0 x 10 <sup>-8</sup> M		1.0 x 10 <sup>-7</sup> M	
[βCD] (M)	Background	Peak	Background	Peak
1.00 x 10 <sup>-4</sup>	-	-	-	-
1.00 x 10 <sup>-3</sup>	0.026	0.027	0.026	0.027
7.00 x 10 <sup>-3</sup>	0.027	0.030	0.026	0.030
1.05 x 10 <sup>-2</sup>	0.027	0.031	0.026	0.043
[ANS] (M)	1.0 x 10 <sup>-6</sup> M		1.0 x 10 <sup>-5</sup> M	
[β-CD] (M)	Background	Peak	Background	Peak
1.00 x 10 <sup>-4</sup>	0.029	0.031	0.050	0.055
1.00 x 10 <sup>-3</sup>	0.029	0.033	0.050	0.081
7.00 x 10 <sup>-3</sup>	0.029	0.044	0.050	0.154
1.05 x 10 <sup>-2</sup>	0.029	0.050	0.050	0.211
[ANS] (M)	1.0 x 10 <sup>-4</sup> M		1.0 x 10 <sup>-3</sup> M	
[β-CD] (M)	Background	Peak	Background	Peak
1.00 x 10 <sup>-4</sup>	0.204	0.308	0.672	0.768
1.00 x 10 <sup>-3</sup>	0.204	0.572	0.672	1.472
7.00 x 10 <sup>-3</sup>	0.208	1.776	0.704	4.203
1.05 x 10 <sup>-2</sup>	0.208	2.112	0.672	5.120

<sup>a</sup> Peak height was measured for each solution.

## Appendix 9

Retention times of HP- $\beta$ -CD in the presence of t-butanol<sup>a</sup>

[t-butanol] M		$t_1$ (min)	$t_2$ (min)	$t_3$ (min)	$t_{av}$ (min)	$1/k'$
0.438	$t_r$	15.88	15.99	15.86	15.91	$0.338 \pm 0.002$
	$t_0$	4.03	4.02	4.02	4.02	
0.417	$t_r$	15.86	15.63	15.45	15.65	$0.350 \pm 0.005$
	$t_0$	4.05	4.05	4.08	4.06	
0.396	$t_r$	17.58	17.63	17.68	17.63	$0.309 \pm 0.001$
	$t_0$	4.16	4.18	4.17	4.17	
0.354	$t_r$	18.40	18.87	18.98	18.75	$0.299 \pm 0.005$
	$t_0$	4.33	4.31	4.31	4.32	
0.292	$t_r$	18.88	18.93	18.83	18.88	$0.278 \pm 0.001$
	$t_0$	4.12	4.09	4.13	4.11	
0.188	$t_r$	24.23	24.37	24.53	24.38	$0.249 \pm 0.002$
	$t_0$	4.86	4.88	4.87	4.87	

<sup>a</sup>Detected at excitation wavelength of 368.0 nm and emission wavelength of 468.0 nm, using a  $C_{18}$  column and mobile phase containing  $1.0 \times 10^{-4}$  M ANS at a flow rate of 1.0 ml/min. See section 3.2.3.2 for further details.